UNIVERSITY OF BATH

FINAL YEAR MENG PROJECT REPORT

Wave energy converter power increase through active control: Fixed Gains

Carl Selig

supervised by

Dr. Andrew HILLIS

assessed by

Dr. Joseph FLYNN

May 13, 2020

Summary

This report presents work performed in the field of Wave Power, a promising source of renewable energy. It concerns the development and investigation of a control system for a type of device known as a Wave Energy Converter. The specific device which is considered is known as WaveSub[1] and consists of a submerged float tethered to a platform which extracts power from passing waves.

In previous work a control strategy known as Simple and Effective control [2] was adapted for use with a simulated model of the WaveSub device. However, a drifting problem was observed where the device would deviate from its home position over time, exceeding the constraints of the device. If this were to happen in real life the device may be damaged.

This project methodically recreates the Simple and Effective control strategy for the device, seeking to reproduce this drifting problem. The problem was re-created.

Methods of resolving the issue were investigated. Some evidence was found to suggest that the issue was caused by a flaw in the constraints of the Simple and Effective control strategy. An integral feedback loop was added that successfully eliminated the drifting problem in a simplistic simulation environment.

Finally the power generation of the device was compared to a passively damped, optimally tuned control strategy and found to generate more power in gentle sea-states, but less power in violent sea states. The largest percentage increase in power was 162.2%, whilst the biggest decrease was 11.0%.

Overall the method was found to have promise, but further research is required before recommendations on physical experimentation can be made.

Acknowledgements

I would like to thank Dr. Andrew Hillis for going above and beyond the role of supervisor.

I also wish to thank my family and friends for providing support and a significant amount of proof reading.

Finally I thank my therapist, Laura Keyte, for private reasons.

Contents

List of Figures

List of Tables

Nomenclature

DOF Degree(s) of Freedom

IMC Internal Model Control

$MATLAB$ Matrix Laboratory. A programming language and development environment specialised for the manipulation of matrices.

$MIMO$ Multiple Input Multiple Output

$Plant$ The physical system which is being controlled

$Simulink$ A graphical programming environment based on MATLAB. Users manipulate dynamic systems by placing and connecting blocks.

$SISO$ Single Input Single Output

WEC Wave Energy Converter

Chapter 1

Introduction

Wave power refers to a group of technologies that harvest energy from sea waves. It is distinct from Tidal power. Wave power is relevant as a renewable energy source that has advantages over other sources such as solar and wind. Most notably, it constantly produces a base amount of power; can be used along most coastlines; and has a low initial expenditure. [7]

This report seeks to present the results of the research project conducted by the Author as well as the means to reproduce them. The project is part of a larger research effort to increase the power generation of Wave Energy Converters (WECs) through control system design. It is hoped that improved power generation will increase the commercial viability of the field. Wave power is already considered a viable energy source for the UK [7] but has not seen widespread commerical adoption at the time of writing [3].

There have been two WEC projects in the UK that have reached commercialisation. Pelamis from Pelamis Wave Power and Oyster from Aquamarine Systems[3]. Figure 1.1 shows these devices as they were installed. Pelamis 1 was installed in 2004 and became the first WEC to provide power to a National Grid. Pelamis 2 became the first WEC to be purchased by a utility company in 2009. Oyster was installed in 2012. Both devices provided power to the National Grid over the course of their lifetimes.

Figure 1.1: Pelamis 2 (Top) and Oyster (Bottom) as installed at the Billia Croo wave test site in Orkney, Scotland [3].

According to the Carbon Trust [7] the development of a WEC with improved power generation performance and lower initial costs would positively affect the adoption of the technology in the UK.

One way of achieving these goals is to use a control system. In this project an in-development WEC known as WaveSub[1] is used to investigate the effectiveness of a computationally cheap control scheme that, if successful, may fulfil both requirements.

The WaveSub device consists of a submerged cylindrical float tethered to an underwater platform via 4 cables[1]. The cables drive Power Take Offs (PTOs) that can extract energy from the motion of the float relative to the platform [1]. In this project these PTOs are modelled as cable drums.

A model of the Wave Sub device has been produced in prior work by A. Hillis, the project supervisor [6]. Figure 1.2 shows a published graphic[1] of this device against the modelled WEC[6]. It was chosen as a generic example of a multi-DOF WEC. The Carbon Trust describes multi-DOF WECs as being of particular interest to UK energy infrastructure due to their increased potential for energy capture over single DOF WECs [7].
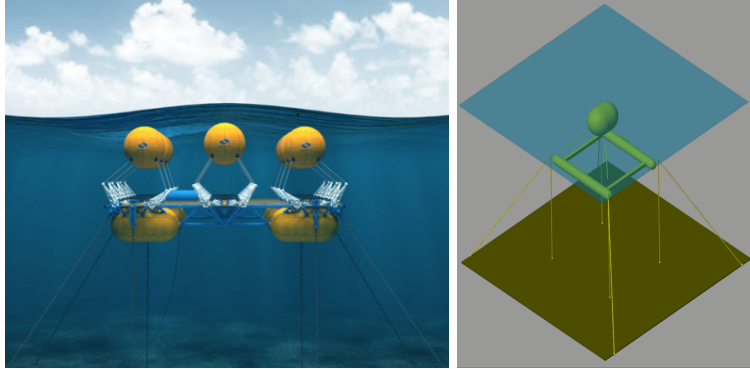
Figure 1.2: A graphic of an array of 9 WaveSub devices(left)[1] versus the modelled WEC(right). Note that cable arms exist in the left figure but are absent in the right due to divergent design.

The model shown in figure 1.2 was created using a simulation environment known as wecSim[8] which was originally developed by a collaboration with the US department of Energy, and then adapted for use with the WaveSub device by Marine Power Systems and associates. [1].

This simulation was used in prior works by Dr. Hillis to compare the power extraction of a Model Predictive Control (MPC) scheme to an, "Optimally tuned, passively damped," system [6]. This approach was also used in this project to assess control system performance.

Many control schemes have been used to increase the power absorption of the WaveSub device and other WECs such as floating-point absorbers [9][10]. Of note is a scheme known as, "Simple and Effective" control proposed by John Ringwood and Francesco Fusco [2]. They claim that this scheme approaches the effectiveness of an MPC scheme whilst being both simpler and more robust. The claim of having advantages over MPC is attractive since MPC is considered an industrial standard due to its ubiquity in digital controllers [11]. MPC schemes are straightforward to implement and can optimise for the present time period whilst also considering future input. They are understood well enough that they can often be redesigned "on the fly," [11]. Both control schemes rely on a model of the system. In the case of Simple and Effective control the system uses an analytical model to predict Wave Excitation Force. This is taken as an input, then passed to an Extended Kalman Filter and an adaptive law based on wave peak frequency to evolve an optimal velocity trajectory. The control system then subjects the WEC PTO to Proportional-Integral control in order that the prime mover(float) tracks the velocity trajectory. The block-diagram for this scheme is reproduced below in figure 1.3.
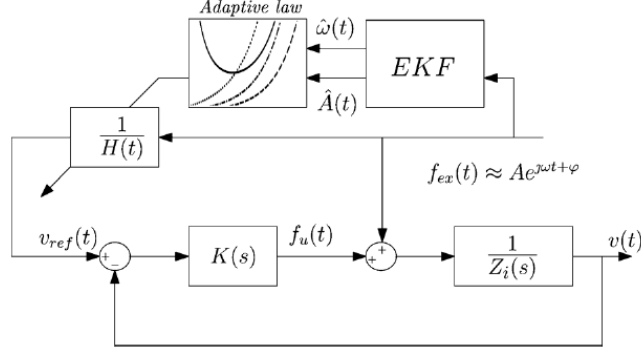
Figure 1.3: Reproduction of figure 3 from "A Simple and Effective Real-Time Controller for Wave Energy Converters," [2]

Shown are the estimated Wave Excitation Force input, $f_e x$ (t); the Extended Kalman Filter (EKF) and Adaptive law implementation. Wave Excitation Force is estimated as sinusoidal. The Simple and Effective control scheme therefore offers a significant advantage over more computationally intensive methods, including MPC. However, these results have only been shown to be true for single DOF WECs. In unpublished work, Hillis has implemented this control scheme in a 6 DOF system[6]. He has observed that the float drifts from its home position over time, eventually violating the device's constraints.

This project presents a methodical re-creation of Hillis' work, and shows that this drifting problem most likely arises due to flawed assumptions in the Simple and Effective control scheme. A potential resolution to the problem is proposed and power generation compared to a passively damped, optimally tuned system is examined.

Chapter 2

Literature Review

The modern concept of wave power was first proposed in 1974 by Stephen Salter in the form of the self-styled Salter duck [4]. This device was proposed as an alternative to oil during the 1973 Oil Crisis in the UK. As shown in Figure 1 the Salter duck generates power by having its vane, or beak (a) bobbed by incoming waves. This produces an oscillation which is transferred to an internal drum(h) via a ratchet(c and d). This turns the bobbing motion caused by the waves into rotary motion which can be used to generate power. Note that the water level (e) is lower behind the device as energy has been removed from the wave.

Salter is considered a foundational figure in the sector [11]. So it is only fitting that the first piece of literature to be considered is his own account of his work. It is titled "Wave Power: Nostalgic Ramblings, future hopes, and heretical suggestions" [12].

Despite the humorous title and less than perfectly rigorous approach, this report provides a factual account of the beginnings of the field. Opinion is not always clearly stated, so care must be taken by the reader to separate the conjecture from the history. The scientific descriptions of the device, however, are clear and accurate. This makes the work a good introduction to the subject area.

As a brief summary, Salter received funding from the UK Department of Energy to set up a laboratory in Edinburgh. Wave power then garnered interest from other British academics, notably David Evans in Bristol who invented the Bristol Cylinder [13]. Evans also developed theories on the hydrodynamics and efficiency of WECs under idealised conditions [14]. His work concerns a one-dimensional scenario where waves are modelled as perfect sinusoids that meet the WEC at right angles. This is not the case in nature and thus his claim that 100% extraction of wave energy is possible has never been produced in practice.
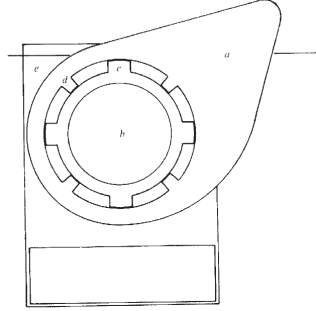
Figure 2.1: A reproduction of a figure from "Wave Power,"[4]. "a. vane; b, a hollow cylindrical member; c, paraxial ridges; d, inward facing ridges on the vane; e, vertical fin between this vane and the next."

Unfortunately, with the conclusion of the Oil Crisis, Salter and Evans found it increasingly difficult to secure funding for their research and none of their devices have been brought to market. In his report, Salter blames pressure from the nuclear sector and "others [who] set out to destroy what they saw to be a threat," [12]. He then goes on to explain that whilst WECs were initially billed as very simple the reality is significantly more complex.

To understand just how complex the field has become it is necessary to review works that represent the state of the art in the field. Many researchers in the field, including this projects' supervisor A. Hillis, have presented their work at the European Wave and Tidal Energy Conference (EWTEC) [6][15][16][9]. The most recent conference proceedigns have therefore been taken as source of state of the art research[17].

The proceedings are generally professional and clear. Although it appears there has been comparatively little work on multi-DOF WECs compared to more constrained devices. In general the field has become far more practical since Salter and Evans' time, with papers such as "Wave Excitation Force Estimation for Wave Energy Converters of the Point-Absorber Type" [16] examining practical limitations of sensors and experimental results in detail.

There is a single piece of literature that underpins the majority of this project. It is titled "A Simple and Effective Real-Time controller for Wave Energy Converters" by Fusco and Ringwood [2]. This paper presents the Simple and Effective control strategy discussed in the Introduction. It is particularly well written, concisely providing all the information needed to reproduce the control system. This Simple and Effective control system is shown to produce near-maximal power generation in a 1 DOF WEC whilst being computationally cheap. As mentioned this is a highly desirable result [7].

This work was previously singled out and recreated by this project's supervi-

sor, A. Hillis. He attempted to adapt it to the WaveSub device, but discovered that the float exhibited a drift from its home position, eventually violating the physical constraints of the system. This work seeks to review this work and determine whether this drift problem is the result of Hillis' implementation, an incompatibility of the control strategy with the WaveSub Device, or a flaw in Ringwood's work.

Chapter 3

Aims and Objectives

The aims of this projected are phrased as 3 research questions.

1. Does a drift problem occur if Ringwood's Simple and Effective Control strategy is adapted for planar motion?

2. If the drift problem exists, can it be resolved?

3. How much power does this implementation generate compared to an optimally tuned, passively damped system?

To answer these questions, it was necessary to achieve the following objectives.

1. Reproduce Ringwood's Simple and Effective control system for a planar model and regular sea-states.

   (a) Find a way to create an inverse of the State-Space model of the WEC

   (b) Create an Internal Model Controller (IMC) and verify that it can make the state-space model track simple signals such as sine waves.

2. Adapt the control system for use with irregular sea states.

   (a) Produce look-up tables from bode plots of the radiation transfer functions.

   (b) Implement the adaptive law of the Simple and Effective control method [2].

   (c) Implement the Extended Kalman Filter and tune it using sea-states generated by WecSim.

(d) Implement the position constraints using conditional Simulink logic blocks.

3. Record the Results of the Simple and Effective Control Scheme and answer research question 1.

4. Implement an integral feedback loop

5. Record the results and answer research question 2.

6. Tune the system and produce final results.

7. Answer research question 3.

8. Produce the Final Report

Previously this list included an objective to implement the controller within the WecSim environment. Unfortunately this could not be completed until the very end of the project due to the reasons discussed in section 7.2. The results from the previous objectives were researched instead.

Chapter 4

Research Methodology

This research seeks to confirm the drift result previously produced by the project supervisor, Dr. Hillis. It makes use of much of his work as a foundation but seeks to reproduce his findings using independent work. By reviewing in this way it is hoped that a greater understanding of the Simple and Effective control method as it applies to multi-DOF WECs can be reached.

4.1 Positivism and Simulation

This research makes use of a positivist approach wherein hypotheses are proposed and then either refuted or not-refuted by physical evidence. This project is also a simulation-based project, and thus does not produce physical evidence.

This contradiction is resolved by the understanding that a simulation can produce results that are representative of results in the real world. This is supported by experience with well-estabished models such as the Pierson-Moskowitz Spectrum relation[18] which has been extensively reviewed[19] and found to be representative of reality.

Well-established models are not always available. Less well established models such as the State-Space model of the float [6] are used as well as novel inventions. These cases are clearly stated and the simplifying assumptions used to produce them are catalogued in section 5.1. Since the author creates both the system and its test it is possible to inadvertently bias results by disproportionately including or excluding assumptions that increase the likelihood of significant results. Whilst every effort is made to be rigorous this bias can only truly be eliminated through experimental verification.

Physical verification is not required unless a significant result has been found. For this and other practical reasons real world experimentation is outside of the scope of this project. If significant results are found then this project will serve as an inexpensive precursor to physical testing. If significant results are not found then physical testing may be applied more fruitfully elsewhere. Historically, simplifying assumptions have made significant simulation results easier to produce[19]. This suggests that the failure to find significant results makes a strong case that there is nothing to be found from further research.

4.2 Equipment

The only physical apparatus used in this project was the author's personal computer.

The software used to create and run the simulation was MATLAB R2018b and Simulink 9.3. The licenses for this software were obtained through the University of Bath.

Git and its associated platform Github were used to backup and distribute all project files. A link to the repository is provided in appendix E

The typsetting environment, LATEX, was used to produce this report and other documents.

Chapter 5

Simple and Effective Control

Simple and effective control refers to a strategy presented by Fusco and Ringwood in their paper, "A simple and effective real-time controller for wave energy converters,"[2]. This strategy was designed for a 1-DOF WEC, however the WaveSub device considered in this project is a 6-DOF device. This complicates the implementation of simple and effective control. Simplifying assumptions were made which are described in Section **??**. The most important of these is the assumption that the WaveSub device behaves as a planar device, and that only surge and heave motions are controlled. Therefore the control strategy need only be adapted for 2 DOF, rather than 6.

Figure 5.2 shows the full implementation of the control strategy in the Simulink environment. This chapter will detail each component in sufficient detail that the reader may re-create the system. The input to the system is a 6 element vector of wave excitation forces in each dimension(F_{ex}). The output is 6 element vector of float velocities in the same dimensions. The 6 dimensions and their order in the vector are Surge, Sway, Heave, Roll, Pitch, and Yaw.
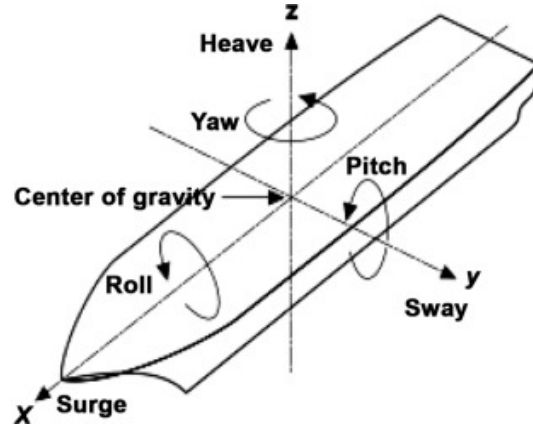
Figure 5.1: The 6 degrees of freedom relative to a boat. For the modelled float shown in figure 1.2 the Yaw axis (y) is coincident with the cylindrical axis of the float. Figure reproduced from "Deepwater Drilling"[5].
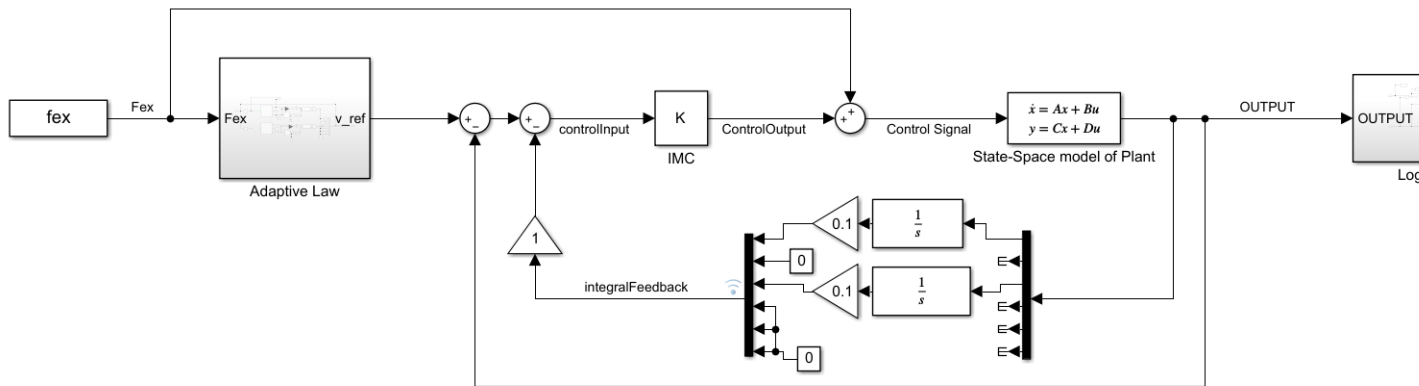
Figure 5.2: The full implementation of simple and Effective Control for the WaveSub device.

5.1   Simplifying assumptions

Sea states are modelled as irregular waves, meaning that they are the finite sum of many simple harmonic (regular) waves. Real life waves can be described perfectly as an infinite sum of regular waves, but this cannot be calculated in real-time. The waves are created from a pseudo-random combination, rather than being based on recorded data.

The energy distribution within a generated irregular wave is modelled using an empirical relationship known as the Pierson-Moskowitz spectrum. The technique is fully described in "A proposed spectral form for fully developed wind seas based on the similarity theory of S. A. Kitaigorodskii," by Pierson and Moskowitz[18]. This spectrum relates wave frequency and energy distribution and is based on the assumption that sea waves are in equilibrium with the wind. A 2003 review paper using modern wave data reaffirmed that "for the chosen data only... [the spectrum] provides statistically robust relations."[19]

It is assumed that most sea waves will be between 0.5 and 6.5 metres in significant height (Hs), and have a period between 6 and 16 seconds. Sea-state samples were created at half metre and whole second intervals in each of these ranges respectively. This is assumed to be representative of all sea states that the WEC would encounter in real life. This is based on the same study performed by Pierson and Moskowitz mentioned above [18].

The float is modelled by a state-space model taken from the project supervisor's unpublished work[6]. In this model it is assumed that the platform holding the PTOs is stationary. In the WECSim environment motion of the platform due to wave excitation force is modelled.

It is assumed that the signal noise that would be generated by real sensors would not significantly affect the performance of the kalman filter and hence the development of the reference velocity. This noise was not modelled in the wave excitation data.

Wave excitation force is assumed to be negligible in all dimensions save for Surge, Heave, and pitch meaning that the float dynamics can be modelled as planar. In addition, cross-terms that relate forces across dimensions are neglected.

5.2   Internal Model Control

Internal Model Control(IMC) involves creating a model of the plant, and then inverting it. The inverse model produces a signal that will reproduce the control
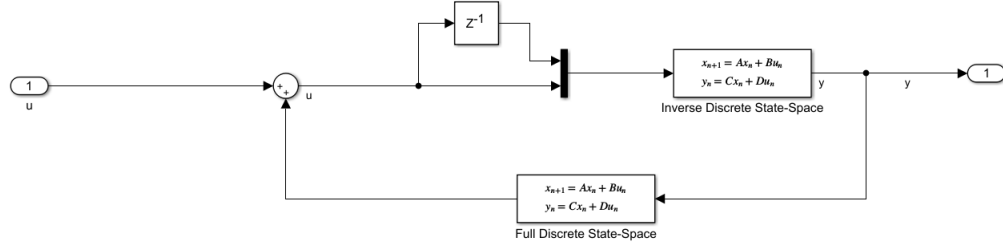
Figure 5.3: IMC implementation using an inverted state space model.

signal when given as input to the plant. This method is reliant on accurate modelling.

Figure 5.3 shows the implemented controller. It is a positive feedback loop, where the forward path is an inverse state-space model of the float, and the feedback path is the state space model. It is implemented as described in Ringwood's paper [2].

The model used is a state space model taken from unpublished work by the project supervisor [6]. Its derivation is outside the scope of this project. It takes 3 input forces and 3 input torques, one for each DOF. It outputs 3 velocities and 3 angular velocities. The inversion of this state space model is novel work, and is detailed in section 5.3 The only change is that the MATLAB command, "c2d" has been used to turn the continuous-time state-space model into discrete-time. Using discrete time also forces the Simulink Solver to use a known numerical method. This prevents errors cause by mismatched solver methods.

5.3   Inverting the state-space model

The desired inverse will map the outputs of the state-space model to its inputs.

One inversion method is to convert the state-space system into a system of transfer functions. In this case the inverse is the reciprocal of the transfer function. This method is complicated by the fact that the plant is a 6x6 MIMO system. Generating corresponding transfer functions using inbuilt MATLAB methods results in 36 high order transfer functions.

This over-fitting of the model can be corrected by manually fitting lower order transfer functions to the system. The project supervisor has used this approach in unpublished work[15]. The results of this work have been provided

for comparison in the Results section.

Another inversion method known as the Massay-Sain algorithm has been used instead. It is able to overcome some of the shortcomings of the transfer function method. It does not require a filter to be stable; it calculates all cross terms; and does not over-fit the model.

The Massey-Sain algorithm was first presented by Sain and Massay in 1969[20]. In 2004 it was summarised in a lecture given by Professor S. Sundaram[21]. The following derivation is paraphrased from Sundaram's lecture and simplified.

First it is necessary to test whether or not the system is invertible. All discrete-time state space systems are of the form

$$x(t + 1) = Ax(t) + Bu(t) \tag{5.1}$$

$$y(t) = Cx(t) + Du(t) \tag{5.2}$$

Where x is the state vector; y is the output vector; u is the input vector; A is the state matrix; B is the input matrix; C is the output matrix; and D is the disturbance matrix.

For our system there is no disturbance input and so D is the zero matrix. It will not be shown in further equations.

From Sundaram, "A system has an inverse with delay L if $u(t)$ can be uniquely determined from $y(t), y(t + 1), y(t + L)$ (and perhaps $x(t)$)."[21] So values of L must be tested to see if $u(t)$ can be uniquely determined.

It is possible to express later time-steps in terms of the current time step via substitution.

$$y(t + 1) = Cx(t + 1)$$

Substituting equation 5.1,

$$y(t + 1) = Ax(t) + Bu(t)$$

This can be iterated for any number of time steps. It can also be represented in a matrix format:

$$\begin{bmatrix} y(t) \\ y(t+1) \\ y(t+2) \\ \vdots \\ y(t+L) \end{bmatrix} = \begin{bmatrix} C \\ CA \\ CA^2 \\ \vdots \\ CA^L \end{bmatrix} x(t) + \left[\begin{array}{c|cccc} 0 & 0 & 0 & \ldots & 0 \\ CB & 0 & 0 & \ldots & 0 \\ CAB & CB & 0 & \ldots & 0 \\ \vdots & \vdots & \vdots & \ddots & \vdots \\ CA^{L-1}B & CA^{L-2}B & CA^{L-3}B & \ldots & 0 \end{array} \right] \left[\begin{array}{c} u(t) \\ \hline u(t+1) \\ u(t+2) \\ \vdots \\ u(t+L) \end{array} \right]$$

$$= Y_{(t,L)} = O_L x(t) + M_L U_{(t,L)} \tag{5.3}$$

Where O_L is analogous to the Observability of the system, and M_L to its Measurability. The partitions show that M_L contains the smaller matrix M_{L-1}. This can be iterated for all versions of M_L down to M_0.

Massey and Sain's theorem[20] asserts that if the rank of M_L minus the rank of M_{L-1} is equal to the number of columns $'m'$ of M_{L-1} then there exists a matrix $\mathcal{K}$ such that

$$\mathcal{K}M_L = \left[\; I_m \mid 0\; \right]$$

Multiplying equation 5.3 by $\mathcal{K}$,

$$\mathcal{K}Y_{t,L} = \mathcal{K}O_L x(t) + u(t)$$

Hence the input $u(t)$ can be expressed in terms of the outputs $Y_{t,L}$

$$u(t) = -\mathcal{K}O_L x(t) + \mathcal{K}Y_{t,L} \tag{5.4}$$

Similarly the state vector at time $t+1$ can be found by substituting equation 5.4 into equation 5.1,

$$x(t+1) = (A - B\mathcal{K}O_L)x(t) + B\mathcal{K}Y_{t,L} \tag{5.5}$$

Equations 5.4 and 5.5 together represent the inverse State-space model.

The task is now to see if there exists a value of L for our system that will satisfy the Massey-Sain theorem. In the case that there are multiple viable values of L the smallest value is preferable as any inverse constructed with it will have the smallest possible delay.

In the case of our 6 input, 6 output system M_0 is the 6×6 zero matrix. It has rank 0, and 6 columns($m = 6$).

M_1 has the form

$$\begin{bmatrix} 0 & 0 \\ CB & 0 \end{bmatrix}$$

where CB is a full-rank 6×6 matrix, making the overall rank 6.

Therefore the system is invertible with $L = 1$ since

$$rank(M_1) - rank(M_0) = m_0$$

As above the matrix $\mathcal{K}$ is formed by performing a pseudo-inverse of M_1 less the last 6 columns. This is done using the pinv() command in MATLAB. This
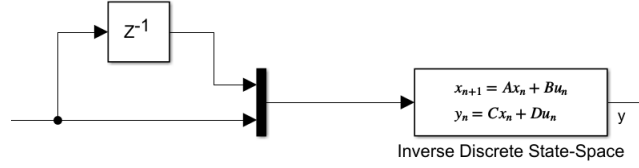
Figure 5.4: The inverted state space model with the a one time-step input delay.

results in a 12×6 matrix. This is expected since

$$Y_{t,L} = Y_{t,1} = \begin{bmatrix} y(t) \\ y(t+1) \end{bmatrix}$$

To find the inverse at the time-step $t+1$ the inverse system must be given both $y(t)$ and $y(t+1)$. since y is a 6×1 vector this makes $Y_{t,1}$ a 12×1 vector which matches the dimensions of $\mathcal{K}$.

The inverse can then be constructed in Simulink, according to equations 5.4 and 5.5, using the discrete state-space block. A one time-step delay is needed to generate $y(t)$ at the timestep $t+1$. This is shown in Figure5.4.

This results in a robust inverse system. When used in the IMC loop it is able to perfectly track simple sinusoid input at a one time-step delay. This delay is negligible for sufficiently small time-steps.

5.4   Adaptive law

Ringwood's paper[2] on Simple and Effective control makes use of an adaptive filter described as $\frac{1}{H(t)}$. This filter takes the dominant frequency and amplitude of the incoming wave excitation force(F_{ex}) and outputs a reference velocity(v_{ref}). The control system then makes the float track this reference velocity as accurately as possible.

Ringwood has shown through extensive study that maximum energy extraction in 1DOF occurs when the float oscillation is in phase with the excitation force's dominant frequency[2]. So to realise maximum energy extraction, "The velocity should always be in phase with the excitation force and it should have an amplitude that is modulated in the frequency-domain by the inverse of double the radiation resistance $\frac{1}{2B(\omega)}$" [2].

This is expanded to cover the two controlled dimensions of the float: Surge and Heave. It is assumed that maximum power extraction may be achieved in both dimensions as they are independent. For example, uneven excitation in these two dimensions will result in elliptical motion of the float.

To construct the filter the radiation response of the float in each dimension must be modelled. The radiation response refers to the forces on the float due to the waves that are generated by the float's motion, and which then carry energy away from the system. These responses can be modelled by transfer functions. The project supervisor has provided these transfer functions and they are shown in appendix A.

These functions transfer float velocity to radiation force. We need to find the amplitude of the radiation response at a given frequency. Bode plots relate the amplitudes and frequencies of systems. Figure 5.5 shows bode plots of both functions.
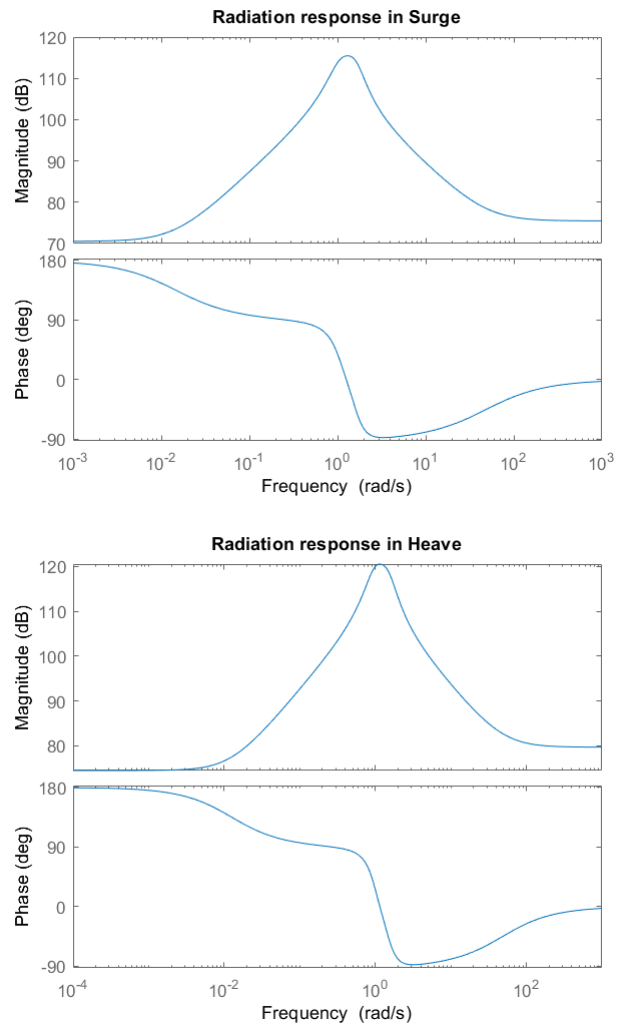
Figure 5.5: Bode plots of the Surge and Heave radiation force transfer functions. Created using the MATLAB bode command.

The data from these plots is then turned into lookup tables to be used in the filter as shown in the code in appendix B. Given the dominant frequency of F_{ex} the radiation amplitude response can be obtained using the lookup table block in Simulink as shown in figure 5.6. According to Ringwood[2] the velocity reference may be obtained via the relation,

$$v_{ref}(t) = \frac{1}{2B(\hat{\omega})} f_{ex}(t)$$

where $\hat{\omega}$ is the radiation force amplitude response produced by the dominant frequency. This is implemented as shown in figure 5.6. Hence v_{ref} is obtained and given as an output.
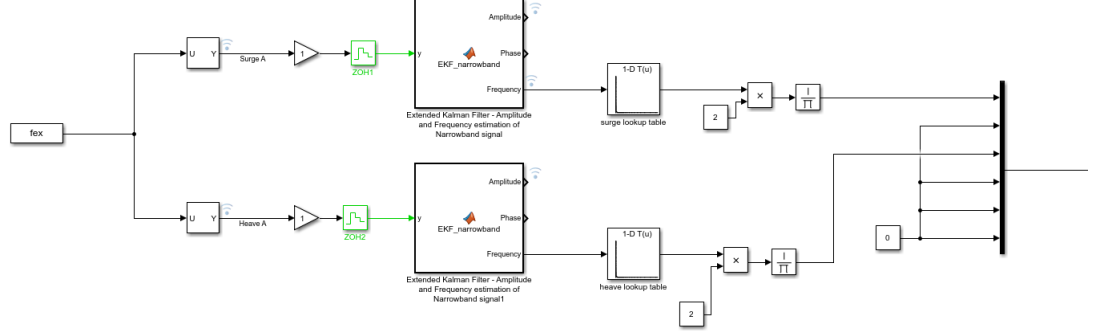
Figure 5.6: The fully implemented adaptive filter in the Simulink environment.

5.5 Filtering Wave Excitation Force

It is necessary to make an estimate of the frequency of F_{ex} in order to produce v_{ref} as described in section 5.4. An extended kalman filter is used to extract these parameters from F_{ex}. The programming of the extended kalman filter block was provided by the project supervisor, and the tuning of it was performed by the author. A copy of the block's code with the tuning parameters used is provided in appendix D

Kalman filters are commonly used in systems where physical processes are well modelled. Physical measurements and predictions are combined in an iterative process to produce more accurate readings than could otherwise be achieved in real time. It relies on data from both processes being normally distributed so that they can be combined simply.

The EKF used in this project is developed from the EKF described by Fusco, F. in his PhD thesis "Real-time Forecasting and Control for Oscillating Wave Energy Devices"[22]. Figure 5.7 shows the filter's estimation of the wave amplitude. Figure 5.8 shows its estimation of the frequency of a sinusoidal wave of frequency 0.1 rad/s.

The estimation of frequency takes more time to reach the correct value than desired. This may have an impact on energy extraction and system stability.

5.6 Constraints Handling

The control strategy has so far only focused on tracking the best velocity for energy capture. There are also physical constraints which must be considered.

29
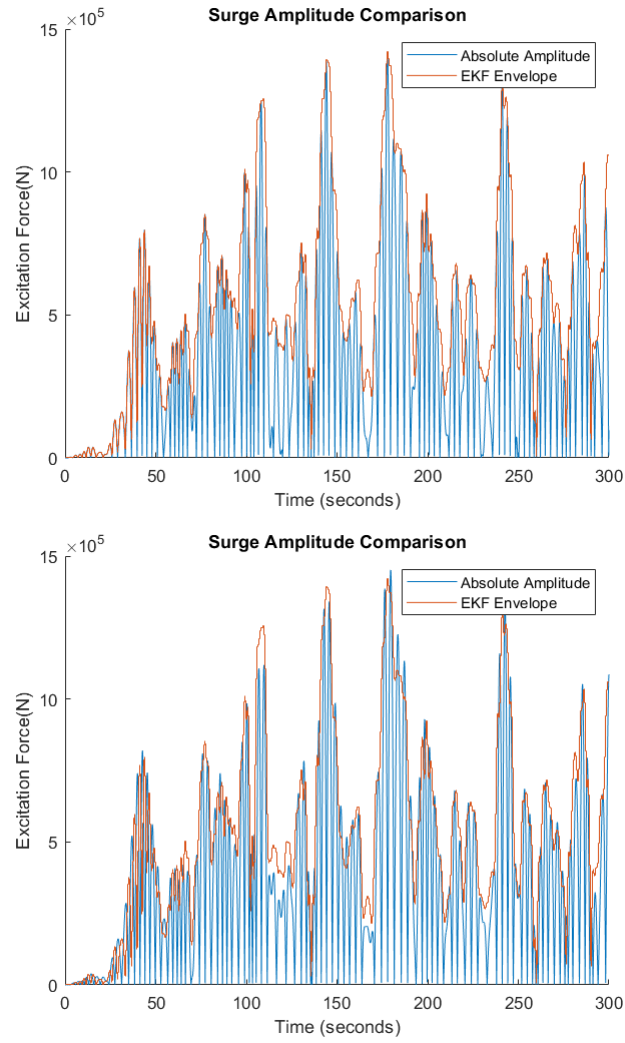
Figure 5.7: Graphs showing the Amplitude Envelope of the EKF compared to
the absolute amplitude of the wave excitation force.
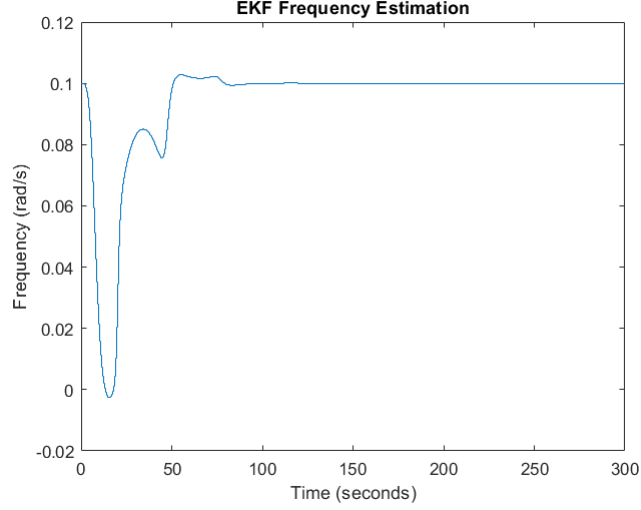
Figure 5.8: Graph showing the EKF estimation of wave frequency. The input is a sinusoid of frequency 0.1 rad/s.

Motions in all of the non-controlled dimensions are already very small and need not be specifically controlled. In the controlled dimensions of heave and surge there are large amplitude motions which may exceed the physical limits of the device.

For the WaveSub device the physical limits in heave and surge are $\pm 5m$ from the home position. A limit of $\pm 3m$ is imposed in the surge dimension as a safety factor. It is important that the float does not crash into the platform.

Ringwood [2] proposes a method to limit the amplitude of the reference velocity, which prevents the float from deviating outside of physical limits so long as the mean of the float's velocity is zero and there is good tracking of the reference velocity. As shown in the results in chapter 6 this is not necessarily the case.

To impose this limit a new term is calculated which can be expressed as,

$$\frac{\hat{\omega} X_{lim}}{\hat{A}}$$

where $\hat{\omega}$ is the frequency of F_{ex}; $\hat{A}$ is the amplitude of F_{ex} in metres; and X_{lim} is the physical limit in the relevant dimension in metres.

The adaptive law from section 5.4 is then modified with conditional logic

31

such that,

$$\frac{1}{H(t)} = \begin{cases} \frac{1}{2B(\hat{\omega})}, & \text{if } \frac{\hat{\omega}X_{lim}}{\hat{A}} > \frac{1}{2B(\hat{\omega})} \\ \frac{\hat{\omega}X_{lim}}{\hat{A}}, & \text{otherwise.} \end{cases}$$

Figure 5.9 shows how this logic was implemented in Simulink.
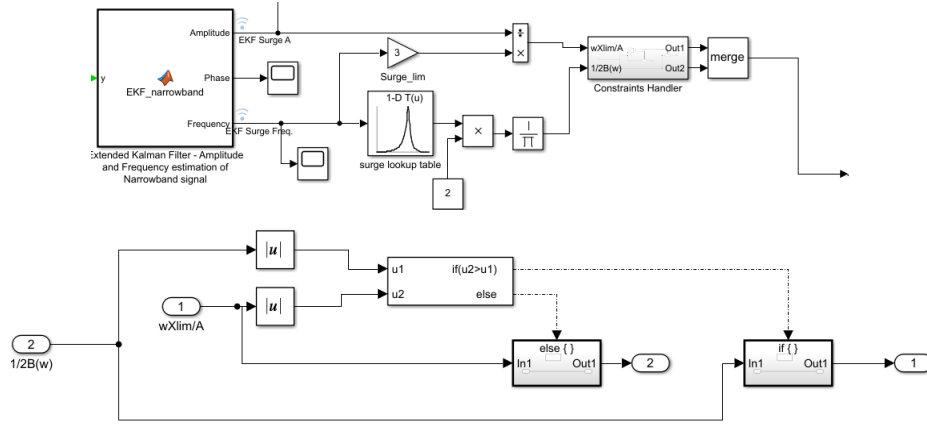
Figure 5.9: Integration with adaptive law(top) and 'Constraints handler' subsystem implementation(bottom).

5.7 Integral feedback

Implementation of the prior sections of this chapter is all that is needed to fully realise Ringwood's Simple and Effective control. However, as shown in the results in chapter 6 this results in a drift that quickly violates physical constraints. This drift may arise due to the fact that the mean of the float's velocity is non-zero. This would mean that limiting the amplitude of the velocity as described in section 5.6 is insufficient.

Introducing an integral feedback loop was investigated as a possible solution. There are many ways to implement this. Figure 5.10 shows one. There are two summing junctions in the figure. Routing the integral feedback path to either one produces a different implementation. There is also a decision to made on whether to use the first or second integral of Velocity.

In this project it was found that the implementation as shown in figure 5.10 produced better power results and better managed the physical constraints.

The gain was tuned with the constraints turned off. It keeps the mean of the velocity to within $0.1ms^{-1}$ of 0. Ringwood's constraints can then be used to limit the velocity, and therefore the position, as intended.
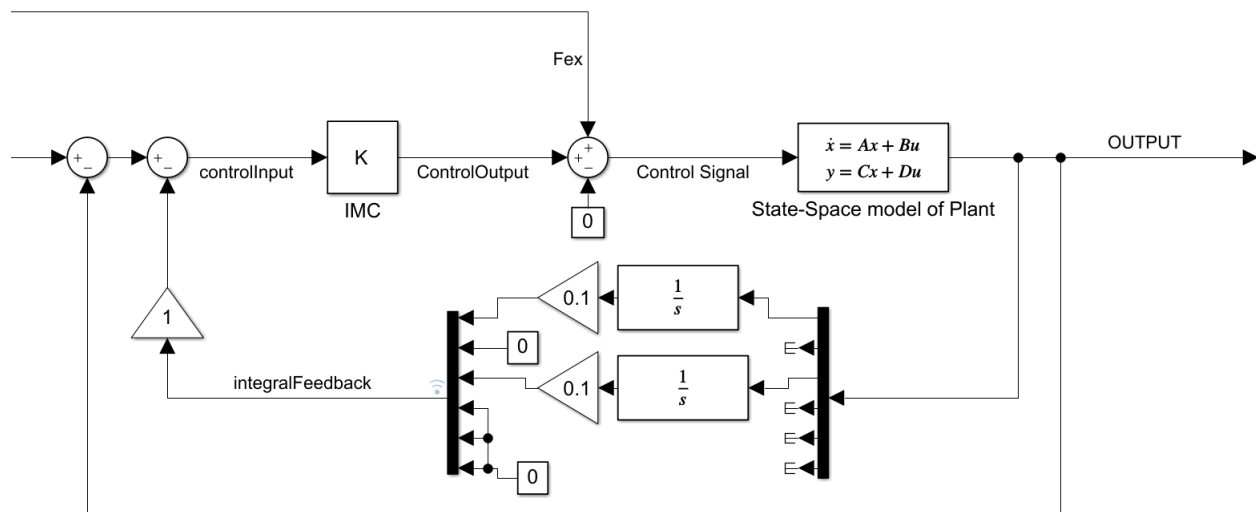
Figure 5.10: One implementation of the integral feedback loop.

Chapter 6

Results

All simulations presented here have been created using wave data generated by WecSim according to the Pierson-Moskowitz spectrum relation [18] with a sampling rate of $\frac{1}{0.02s} = 50Hz$.

The sea states that have been simulated are a combination of two ranges. The range of significant sea heights(H_s) is from 0.5 to 6.5 metres in increments of 0.5m. The range of wave periods(T_e) is from 6 to 16 seconds in increments of 1 second. According to Hillis [6] this is representative of the sea states likely to be encountered by the WEC.

6.1   Tracking Performance

The tracking performance is near ideal save for a delay of one time-step due to the use of the state-space model as the plant. Figure 6.1 shows a typical example of this tracking of reference velocity.

Unfortunately this tracking performance does not carry into wecSim. Figure 6.2 superimposes the float velocity in surge and heave on the reference velocity. The frequencies are identical, but the amplitude of the float velocity is much larger than of the reference velocity.
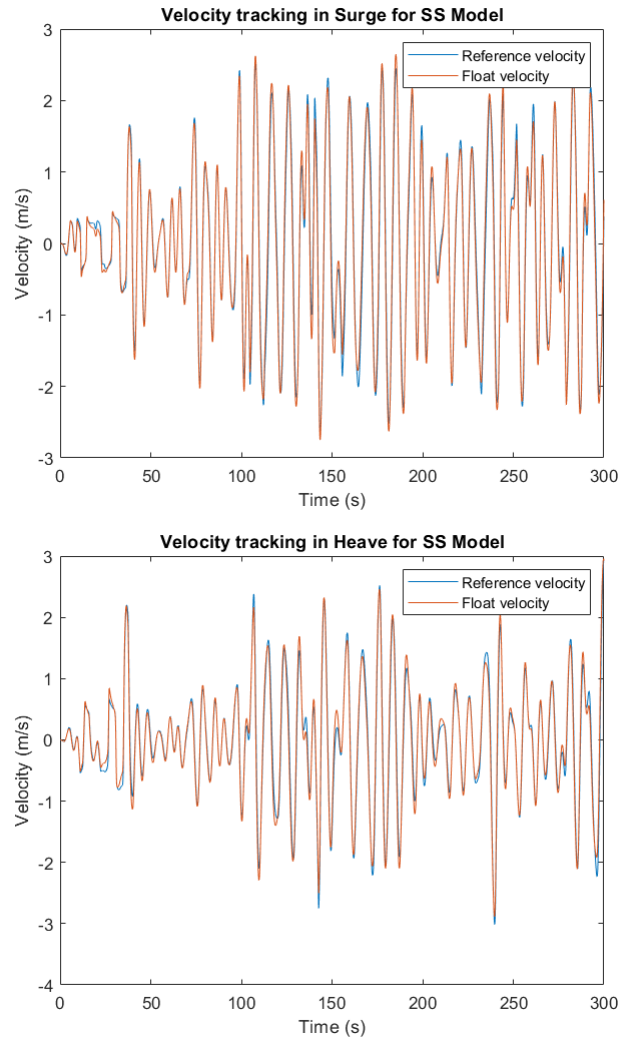
Figure 6.1: Tracking performance of the IMC with the State Space Model as the plant. Hs = 3, Te = 10.
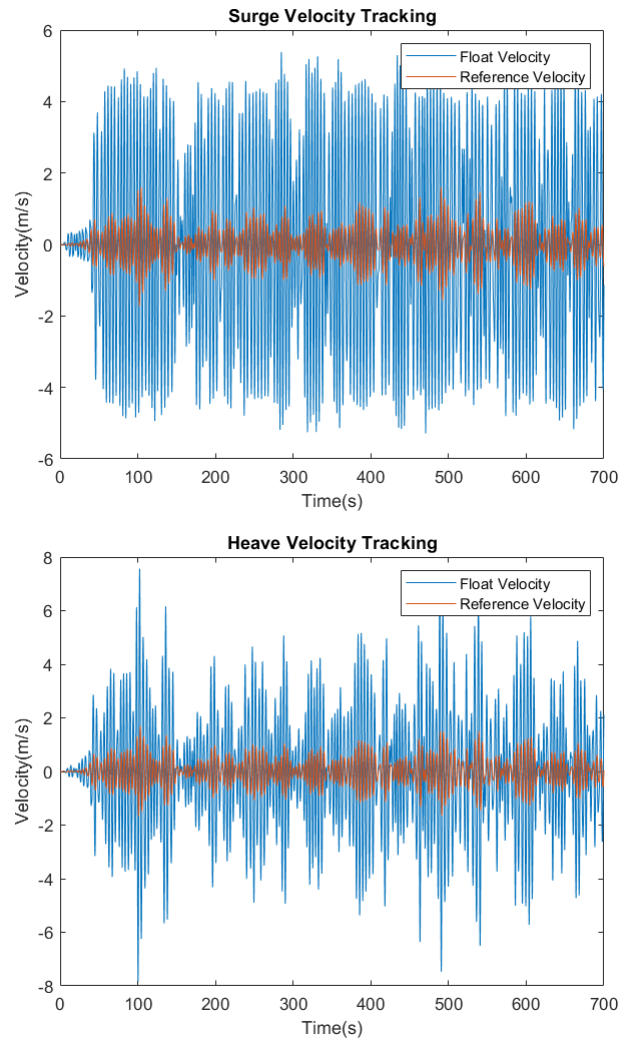
Figure 6.2: Tracking performance of the float in the wecSim environment.

6.2   Power output using State-Space model

The power generated using the Simple and Effective control system is compared against the power generated by an optimally tuned passively damped system as described in "Active control for multi-degree-of-freedom wave energy converters with load limiting" [6].

This passive-damping system relies only on a damping co-efficient that relates cable velocity to cable tension. i.e.,

$$\text{Cable Tension} = \text{Cable Velocity} \times \text{Damping Co-efficient}$$

in the axis of each cable. The co-efficient is optimally chosen for each wave period. This could feasibly be performed in reality using an adaptive law and a method of measuring the sea-wave frequency such as the EKF method described in section 5.5.

Table 6.1 shows the mean power generated in each sea state by the passively damped system. This table is reproduced from unpublished work by A. Hillis [6].

	Mean Power in each Sea State over 700s (kW)										
0	0	0	0	0	0	0	0	0	0	0	0
0.5	12.02	15.57	16.36	15.52	14.19	13.27	12.7	12.19	11.44	10.16	8.06
1	48.09	62.3	65.45	62.1	56.77	53.08	50.8	48.75	45.76	40.65	32.26
1.5	108.2	140.17	147.27	139.71	127.74	119.44	114.3	109.68	102.95	91.46	72.58
2	192.36	249.19	261.81	248.38	227.1	212.33	203.19	194.99	183.03	162.6	129.03
2.5	300.56	389.37	409.07	388.1	354.84	331.77	317.49	304.67	285.98	254.07	201.6
3	432.81	560.69	589.07	558.86	510.97	477.75	457.19	438.73	411.81	365.86	290.31
3.5	589.1	763.16	801.78	760.76	695.49	650.26	622.28	597.16	560.52	497.97	395.14
4	769.44	996.77	1047.23	993.52	908.4	849.33	812.78	779.96	732.1	650.41	516.1
4.5	973.82	1261.77	1325.4	1257.43	1149.69	1074.93	1028.67	987.14	926.57	823.18	653.19
5	1202.24	1557.46	1636.29	1552.38	1419.37	1327.07	1269.96	1218.69	1143.91	1016.27	806.41
5.5	1454.72	1884.53	1979.91	1878.38	1717.44	1605.76	1536.65	1474.62	1384.13	1229.68	975.76
6	1731.23	2242.74	2356.26	2235.43	2043.89	1910.98	1828.75	1754.92	1647.23	1463.43	1161.23
6.5	2031.79	2632.11	2765.33	2623.53	2398.74	2242.75	2146.24	2059.59	1933.21	1717.49	1362.84
	6	7	8	9	10	11	12	13	14	15	16

Significant Wave Height (m) (left axis label)

Sea Wave Time Period (s) (bottom axis label)

Table 6.1: Power generated by optimally tuned passive damping. Reproduced from[6].

Tables 6.2 and 6.3 show the mean power generated by the Simple and Effective Control Strategy without an integral feedback loop. Whilst this control strategy does generate power, it does not comply with physical system constraints. Table ?? shows the maximum heave and surge displacements with those beyond physical limits highlighted.

Power is calculated as the product of the control force output of the IMC controller and the resultant float velocity. The mean power is then calculated as the arithmetic mean of the power produced over the 700 second sample time. Power generation is negative by convention. The arithmetic mean is used as opposed to the geometric mean as instantaneous power oscillates between positive and negative.

Mean power produced in each Sea State over 700s (kW)

Significant Wave Height (m)	6	7	8	9	10	11	12	13	14	15	16
0	0.00	0.00	0.00	0.00	0.00	0.00	0.00	0.00	0.00	0.00	0.00
0.5	31.96	29.96	30.25	30.96	27.24	24.73	23.10	19.65	14.54	9.11	4.63
1	78.69	85.46	82.70	75.02	65.46	63.17	64.38	62.80	55.11	45.98	39.58
1.5	147.78	160.82	170.93	175.23	167.59	154.34	138.41	121.06	106.94	96.36	87.97
2	240.30	273.85	285.79	287.67	282.97	265.32	239.54	212.68	186.68	161.44	140.08
2.5	361.88	410.54	434.80	434.48	417.12	389.10	352.88	310.53	265.56	225.94	191.64
3	511.40	580.11	608.20	597.30	570.26	525.89	472.85	409.81	346.46	289.51	242.68
3.5	679.98	769.48	798.95	776.90	728.78	662.60	588.01	497.37	417.42	350.77	293.27
4	877.83	982.37	1004.30	970.22	898.34	804.60	699.45	581.38	481.28	407.98	346.75
4.5	1100.90	1219.20	1228.00	1172.60	1075.80	961.81	822.64	672.75	552.96	464.54	414.69
5	1347.70	1462.90	1461.10	1390.10	1254.00	1125.70	960.42	782.71	635.66	529.98	490.19
5.5	1615.00	1718.80	1705.40	1621.20	1437.10	1299.70	1110.40	910.37	734.07	609.84	570.56
6	1898.30	1995.60	1963.20	1852.60	1636.50	1479.80	1268.80	1048.10	844.84	704.25	655.57
6.5	2194.80	2290.30	2235.00	2090.40	1853.30	1669.90	1432.00	1186.20	964.22	810.81	747.65

Sea Wave Time Period (s)

Table 6.2: Power generated by Simple and Effective control model. Darker red indicates higher power.

Percentage power difference from passively damped system (%)

Significant Wave Height (m)	6	7	8	9	10	11	12	13	14	15	16	AVG.
0	0.0%	0.0%	0.0%	0.0%	0.0%	0.0%	0.0%	0.0%	0.0%	0.0%	0.0%	0.0%
0.5	245.2%	135.7%	91.1%	80.7%	84.6%	78.5%	61.2%	41.8%	26.2%	18.8%	26.4%	124.6%
1	254.9%	157.1%	108.3%	86.3%	79.1%	69.8%	55.7%	38.5%	24.3%	18.1%	26.4%	94.6%
1.5	246.1%	150.5%	112.8%	93.6%	86.6%	74.8%	58.1%	40.0%	25.6%	19.0%	26.8%	83.6%
2	226.1%	144.5%	107.1%	91.4%	83.9%	69.6%	50.5%	32.5%	18.1%	10.7%	16.5%	73.9%
2.5	219.7%	132.9%	96.7%	81.7%	71.1%	54.4%	32.1%	14.5%	3.3%	-1.5%	3.4%	64.9%
3	206.4%	121.3%	87.0%	69.4%	58.0%	39.1%	16.7%	-2.0%	-13.6%	-17.5%	-9.4%	56.5%
3.5	185.4%	110.3%	77.5%	60.7%	47.4%	27.4%	6.3%	-12.5%	-24.7%	-29.3%	-23.4%	49.0%
4	167.5%	98.0%	67.1%	52.2%	38.5%	18.9%	0.2%	-17.5%	-30.6%	-36.2%	-32.0%	42.1%
4.5	154.9%	86.8%	56.7%	42.4%	30.3%	13.4%	-4.1%	-20.1%	-33.8%	-40.2%	-35.5%	35.7%
5	144.4%	76.2%	46.0%	32.5%	22.2%	8.6%	-7.8%	-23.1%	-36.2%	-42.5%	-37.3%	29.9%
5.5	133.1%	65.8%	35.7%	23.4%	14.3%	2.7%	-12.0%	-26.1%	-38.4%	-44.1%	-38.6%	24.4%
6	121.9%	55.9%	27.1%	15.6%	7.1%	-3.1%	-16.4%	-29.4%	-40.5%	-45.8%	-40.4%	19.4%
6.5	111.1%	47.0%	20.4%	8.4%	1.0%	-8.3%	-20.3%	-32.5%	-42.5%	-47.3%	-42.5%	14.8%
AVG.	89.9%	60.7%	53.6%	55.0%	58.3%	55.4%	47.3%	37.6%	30.2%	29.4%	43.2%	51.0%

Sea Wave Time Period (s)

Table 6.3: Percentage differnces in power generated by Simple and Effective control compared to passive damping. Darker red indicates higher difference. Averages have been excluded from this formatting.

Maximum Surge Position (m)

Significant Wave Height (m)	6	7	8	9	10	11	12	13	14	15	16
0	0	0	0	0	0	0	0	0	0	0	0
0.5	1.7	2.7	3.0	2.6	2.2	2.5	2.7	3.0	3.8	4.5	5.1
1	1.5	1.5	2.9	3.5	4.5	4.6	3.8	2.9	3.2	4.1	4.6
1.5	2.2	2.0	2.0	3.2	3.2	3.9	4.0	3.9	3.6	3.5	3.2
2	1.9	3.2	3.1	3.6	4.5	4.1	3.3	3.4	3.8	4.0	4.1
2.5	2.7	3.4	5.0	5.3	5.0	4.7	5.2	5.6	6.1	6.3	6.4
3	3.2	4.9	5.6	6.2	6.2	7.0	7.0	7.6	8.2	8.5	8.5
3.5	3.3	5.4	6.7	6.1	7.7	8.7	9.1	10.2	10.6	10.6	10.5
4	4.3	5.0	7.4	6.6	8.5	10.0	11.1	12.4	13.0	12.6	12.2
4.5	3.9	5.6	6.3	8.2	9.5	10.8	12.5	14.1	14.7	14.5	13.3
5	3.8	7.6	5.9	8.6	11.0	11.7	13.4	15.1	15.9	15.9	14.0
5.5	5.4	8.7	6.9	8.1	12.3	12.3	14.1	15.7	16.8	16.8	14.7
6	6.8	8.7	7.7	8.5	13.1	12.7	14.6	16.2	17.4	17.4	15.3
6.5	7.9	8.2	7.9	9.3	13.1	12.9	14.9	16.9	17.9	17.8	15.8

Sea Wave Time Period (s)

Maximum Heave Position (m)

Significant Wave Height (m)	6	7	8	9	10	11	12	13	14	15	16
0	0	0	0	0	0	0	0	0	0	0	0
0.5	1.2	1.5	1.7	2.2	2.5	2.5	2.3	2.1	2.0	1.8	1.7
1	1.3	1.6	2.0	2.4	3.2	3.5	3.4	3.1	2.6	2.2	2.2
1.5	1.6	1.4	1.7	1.7	1.7	1.9	2.7	3.4	3.6	3.6	3.3
2	1.6	2.0	1.8	1.7	2.2	2.3	2.5	3.0	3.3	3.4	3.9
2.5	1.8	2.0	2.9	2.1	2.5	3.3	3.1	3.3	3.5	3.7	3.8
3	2.3	2.6	3.3	3.5	3.0	3.1	3.8	4.0	3.8	4.0	4.1
3.5	3.5	4.2	4.3	4.1	4.3	3.6	3.2	4.0	4.5	4.5	4.7
4	3.1	4.3	5.0	4.9	4.7	4.6	4.1	3.5	4.3	4.7	5.1
4.5	2.2	3.7	4.8	4.8	4.3	4.6	4.7	4.5	3.9	4.7	5.0
5	2.8	3.3	4.6	4.5	4.9	5.1	4.8	5.1	4.7	4.4	5.1
5.5	3.7	3.9	4.3	5.4	6.3	6.2	5.1	5.3	5.4	5.2	5.0
6	4.4	4.8	5.0	6.9	7.5	7.0	6.3	5.0	5.9	6.0	5.5
6.5	5.1	4.9	5.4	7.9	8.3	7.9	7.2	5.6	6.2	6.8	6.2

Sea Wave Time Period (s)

Table 6.4: Tables showing maximum position deviation in heave and surge. Red indicates that physical constraints have been exceeded.

With the addition of integral feedback control physical constraints are observed as shown in table 6.7. No significant effect on power generation is observed as shown in tables 6.5 and 6.6.

Mean Power in each Sea State over 700s (kW)											
0	0	0	0	0	0	0	0	0	0	0	0
0.5	31.56	34.55	35.14	34.51	33.02	30.96	28.56	25.97	23.42	21.03	18.84
1	102.75	116.42	121.19	120.62	116.5	109.64	101.05	91.55	82.04	73.17	65.32
1.5	219.05	248.52	259.45	259.47	250.16	234.52	214.89	193.66	172.57	152.97	135.49
2	380.75	432.62	450.66	443.98	423.38	392.62	357	319.74	283.17	250.05	220.73
2.5	590.03	668.02	686.48	664.35	624.97	574.78	519.92	463.56	408.79	359.41	316.21
3	845.95	946.5	953.66	911.75	850.75	776.12	699.12	621.52	546.76	479.73	421.32
3.5	1144.9	1255.6	1249.7	1181.9	1094.8	993.61	892.39	792.31	696.66	610.53	535.6
4	1478	1588.9	1566.7	1471.9	1354.4	1225.6	1099.7	975.43	856.59	750.28	657.91
4.5	1837.1	1945.7	1900.9	1778.4	1628.8	1471.3	1318.5	1166.7	1024.7	897.96	787.15
5	2221.4	2325.7	2257.4	2100	1915.9	1726.2	1545.3	1364.3	1197.9	1050.7	921.89
5.5	2628.2	2728.5	2634.6	2436.3	2214	1989.7	1775.2	1566	1375.6	1207.4	1059.7
6	3059.9	3153.2	3028	2784.1	2522.5	2258.7	2007.1	1769.3	1555.7	1366.6	1199.1
6.5	3514.4	3598.1	3435.5	3142.5	2835.6	2530.6	2241.3	1975.4	1738.2	1527.8	1341.8
	6	**7**	**8**	**9**	**10**	**11**	**12**	**13**	**14**	**15**	**16**

Significant Wave Height (m) — Sea Wave Time Period (s)

Table 6.5: Power generated by integral feedback model. Darker red indicates higher power.

Percentage power difference from passively damped system (%)												
0	0.0%	0.0%	0.0%	0.0%	0.0%	0.0%	0.0%	0.0%	0.0%	0.0%	0.0%	0.0%
0.5	162.6%	121.9%	114.8%	122.4%	132.7%	133.3%	124.9%	113.0%	104.7%	107.0%	133.7%	124.6%
1	113.7%	86.9%	85.2%	94.2%	105.2%	106.6%	98.9%	87.8%	79.3%	80.0%	102.5%	94.6%
1.5	102.4%	77.3%	76.2%	85.7%	95.8%	96.3%	88.0%	76.6%	67.6%	67.3%	86.7%	83.6%
2	97.9%	73.6%	72.1%	78.8%	86.4%	84.9%	75.7%	64.0%	54.7%	53.8%	71.1%	73.9%
2.5	96.3%	71.6%	67.8%	71.2%	76.1%	73.2%	63.8%	52.2%	42.9%	41.5%	56.9%	64.9%
3	95.5%	68.8%	61.9%	63.1%	66.5%	62.5%	52.9%	41.7%	32.8%	31.1%	45.1%	56.5%
3.5	94.3%	64.5%	55.9%	55.4%	57.4%	52.8%	43.4%	32.7%	24.3%	22.6%	35.5%	49.0%
4	92.1%	59.4%	49.6%	48.2%	49.1%	44.3%	35.3%	25.1%	17.0%	15.4%	27.5%	42.1%
4.5	88.6%	54.2%	43.4%	41.4%	41.7%	36.9%	28.2%	18.2%	10.6%	9.1%	20.5%	35.7%
5	84.8%	49.3%	38.0%	35.3%	35.0%	30.1%	21.7%	11.9%	4.7%	3.4%	14.3%	29.9%
5.5	80.7%	44.8%	33.1%	29.7%	28.9%	23.9%	15.5%	6.2%	-0.6%	-1.8%	8.6%	24.4%
6	76.7%	40.6%	28.5%	24.5%	23.4%	18.2%	9.8%	0.8%	-5.6%	-6.6%	3.3%	19.4%
6.5	73.0%	36.7%	24.2%	19.8%	18.2%	12.8%	4.4%	-4.1%	-10.1%	-11.0%	-1.5%	14.8%
AVG.	89.9%	60.7%	53.6%	55.0%	58.3%	55.4%	47.3%	37.6%	30.2%	29.4%	43.2%	51.0%
	6	**7**	**8**	**9**	**10**	**11**	**12**	**13**	**14**	**15**	**16**	**AVG.**

Significant Wave Height (m) — Sea Wave Time Period (s)

Table 6.6: Percentage differnce in power generated by Simple and Effective control with integral feedback compared to passive damping. Darker red indicates higher difference. Averages have been excluded from this formatting.

43

Maximum Surge Position (m)

Significant Wave Height (m)	6	7	8	9	10	11	12	13	14	15	16
0	0	0	0	0	0	0	0	0	0	0	0
0.5	1.1	1.8	1.9	1.8	1.8	1.8	1.7	1.7	1.8	1.9	2.0
1	1.6	1.5	2.5	2.5	2.5	2.8	2.6	2.3	2.5	2.5	2.3
1.5	1.6	1.9	1.8	2.5	2.8	2.9	2.8	2.7	2.8	2.7	2.8
2	1.6	2.1	2.5	3.1	3.3	3.2	3.2	3.2	3.1	3.2	3.2
2.5	2.1	2.7	3.1	3.5	3.2	3.5	3.6	3.7	3.5	3.4	3.5
3	2.6	3.1	3.4	3.3	3.6	3.9	3.7	3.5	3.4	3.6	3.7
3.5	3.0	3.3	3.6	3.3	4.0	3.9	3.7	3.7	3.8	3.8	3.9
4	3.3	3.4	3.6	3.7	4.3	3.9	4.1	4.2	4.2	4.1	4.1
4.5	3.6	3.5	3.7	3.9	4.3	4.3	4.5	4.5	4.5	4.4	4.4
5	3.6	3.6	3.9	4.2	4.2	4.7	4.6	4.6	4.6	4.6	4.6
5.5	3.6	3.7	4.0	4.3	4.4	4.9	4.6	4.6	4.7	4.8	4.8
6	3.7	3.9	4.1	4.4	4.7	4.9	4.6	4.6	4.7	4.9	4.9
6.5	3.7	4.0	4.2	4.5	5.0	4.9	4.6	4.6	4.7	4.9	5.0

Sea Wave Time Period (s)

Maximum Heave Position (m)

Significant Wave Height (m)	6	7	8	9	10	11	12	13	14	15	16
0	0	0	0	0	0	0	0	0	0	0	0
0.5	1.1	1.2	1.3	1.3	1.4	1.4	1.4	1.5	1.5	1.5	1.5
1	1.2	1.3	1.2	1.7	2.1	2.1	1.9	1.7	1.6	1.5	1.5
1.5	1.2	1.2	1.6	1.5	1.5	1.9	2.3	2.4	2.3	2.1	1.9
2	1.4	1.3	1.2	1.7	1.8	1.7	1.9	2.2	2.4	2.5	2.5
2.5	1.8	1.4	1.5	1.8	2.0	2.1	2.1	2.1	2.2	2.4	2.6
3	1.7	1.6	1.8	2.3	2.6	2.6	2.5	2.4	2.4	2.4	2.6
3.5	2.2	2.0	2.1	2.8	3.0	3.0	3.0	2.8	2.8	2.8	2.8
4	2.2	2.0	2.4	3.1	3.2	3.3	3.3	3.2	3.2	3.2	3.2
4.5	2.0	2.3	2.8	3.2	3.4	3.6	3.5	3.5	3.5	3.5	3.5
5	2.2	2.7	3.2	3.4	3.7	3.7	3.8	3.7	3.6	3.6	3.6
5.5	2.4	3.0	3.6	3.5	3.8	3.9	3.9	3.9	3.8	3.7	3.7
6	2.6	3.3	3.8	3.8	4.0	4.1	4.1	4.0	4.0	3.9	3.9
6.5	2.9	3.6	4.0	4.0	4.1	4.1	4.2	4.1	4.1	4.0	4.1

Sea Wave Time Period (s)

Table 6.7: Tables showing maximum position deviation in heave and surge for the integral feedback control model. Physical constraints were not exceeded in any case.

6.3   Power output of wecSim model

Due to difficulties discussed in section 7.2 the control system was only crudely implemented in the WecSim environment. Figure 6.3 shows this implementation.

Some small amount of power was generated by the device despite the poor tracking shown in figure 6.2. Constraints were violated in many sea states due to the increased amplitude of the float velocity in surge.
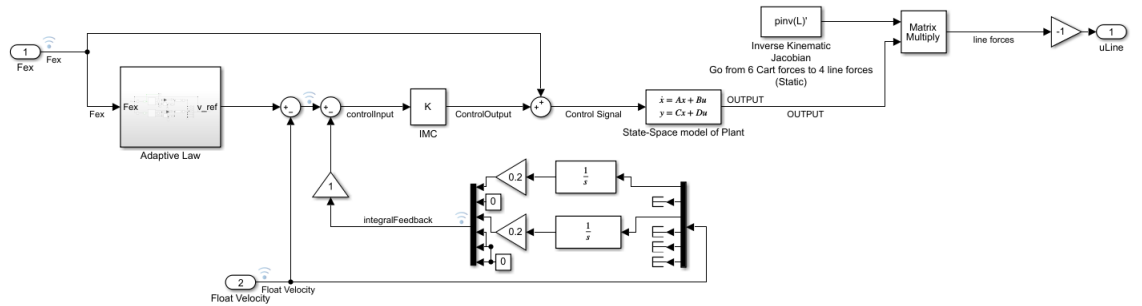
Figure 6.3: The implementation of the integral feedback control system in the WecSim environment.

		Mean Power in each Sea State over 700s (kW)										
		6	7	8	9	10	11	12	13	14	15	16
	0	0.00	0.00	0.00	0.00	0.00	0.00	0.00	0.00	0.00	0.00	0.00
	0.5	0.01	0.01	0.02	0.02	0.01	0.01	0.01	0.01	0.01	0.00	0.00
	1	0.02	0.04	0.45	0.05	0.04	0.03	0.02	0.02	0.01	0.01	0.01
	1.5	0.05	0.08	0.09	0.09	0.07	0.05	0.04	0.03	0.02	0.02	0.01
	2	0.07	0.12	0.14	0.12	0.09	0.06	0.04	0.03	0.03	0.02	0.02
Significant	2.5	0.10	0.16	0.18	0.15	0.10	0.08	0.06	0.04	0.03	0.02	0.02
Wave	3	0.13	0.21	0.22	0.20	0.15	0.11	0.08	0.05	0.04	0.03	0.02
Height (m)	3.5	0.15	0.25	0.26	0.24							
	4		0.28	0.29								
	4.5		0.30	0.34								
	5		0.32	0.38								
	5.5		0.41									
	6		0.42									
	6.5		0.47									

Sea Wave Time Period (s)

Table 6.8: Table showing mean power produced by the crude WecSim implementation. Missing values are due to constraints violation.

46

Chapter 7

Discussion

In place of the WecSim environment, the state-space model used for development of the IMC was used to produce most results. This is undesirable since it makes more assumptions than the WecSim environment, and is identical to the model used in the IMC. The highly accurate tracking produced using this model is therefore unsurprising.

When implemented in the WecSim environment the tracking is worse. As shown in figure 6.2 whilst the frequency of the floats' velocity matches that of the reference signal its amplitude does not. It appears by simple inspection that the amplitudes may be proportional, but this has not been properly investigated due to the constraints discussed below in section 7.2.

One potential explanation for this amplitude difference is that the amplitude response of the controller at high frequencies is large. Figure 7.1 shows the surge-surge and heave-heave responses of the IMC controller. The tested range of sea wave frequencies is between 0.4 rad/s ($Te = 16$) and 1 rad/s ($Te = 6$). In this range the bode plot reveals that the amplitude response grows exponentially with frequency. This implies that the controller produces a large response to high frequency signals which may be inappropriate. These frequencies may be present in the WecSim environment but not the state-space model environment due to WecSim's modelling of high frequency responses such as radiation forces. This problem could possibly be resolved with the use of a high-pass filter. One possible expression of this filter is as a transfer function,

$$\frac{\text{Output}}{\text{Input}} = \frac{s}{s + 2\pi}$$

where 2π is the cut-off frequency. This corresponds to 1 Hz which is the

upper bound on typical sea-wave frequencies [19].

Another potential explanation is that the Massay-Sain IMC features a real-time delay where Dr. Hillis' system does not. When transforming to the frequency domain a real-time delay becomes an exponential term. For example, if a function $f(t)$ is shifted by time a,

$$\mathcal{L}[u(t-a)f(t-a)] = e^{-as}F(s)$$

. This exponential term could be responsible for the large amplitude response.

Signal properties that are present in WecSim but not the State-Space model environment are examples of model error. It was hoped that this model error would be insignificant as detailed in section 5.1. This was mistaken. This implies that this implementation of Simple and Effective control is not robust to model error.
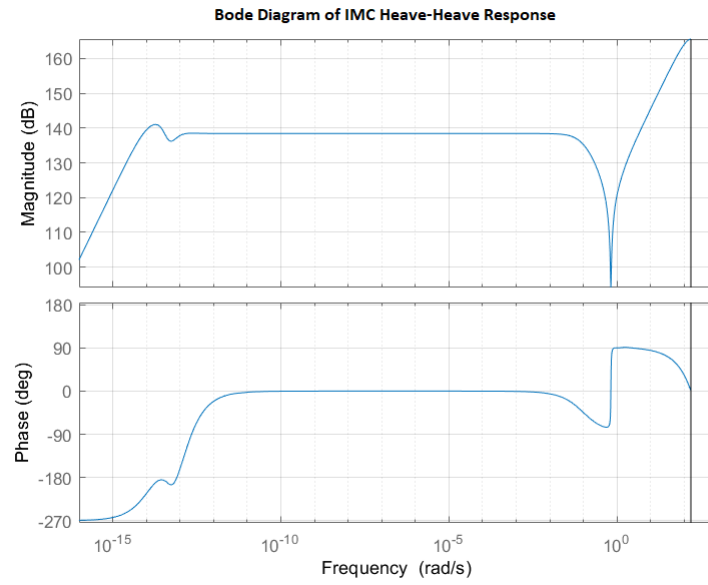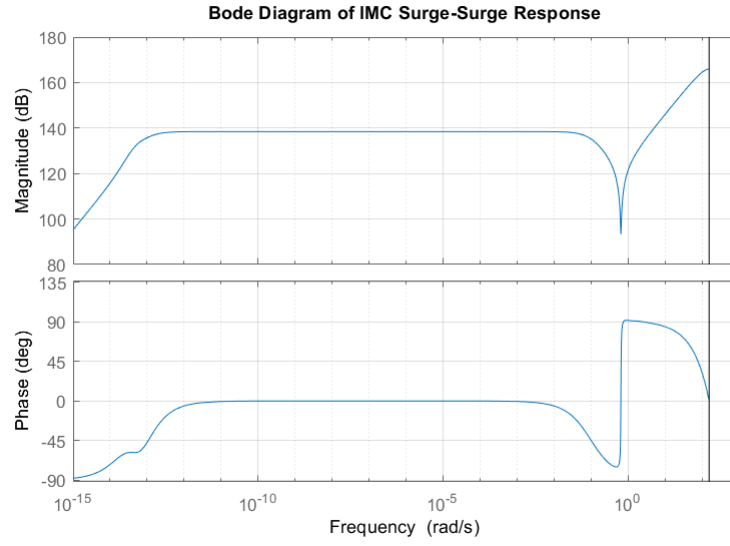
Figure 7.1: Bode plots showing the surge-surge(top) and heave-heave(bottom) responses of the IMC controller.

7.1 Suitability for review

Overall it has been demonstrated that the Massay-Sain inverse State-Space model is robust for practical purposes. It was stable for all tested sea-states in both environments. Whilst the controller's response in the WecSim environment is too large, it is still finite.

Whilst imperfect, this implementation of the IMC is suitable for the purposes of review. It is robust and produces good tracking whilst being distinct from the IMC developed by A. Hillis, which uses transfer function approximations.

By extension the entire implementation of Simple and Effective Control is suitable for review. It is a reproduction of the same methodology described by Ringwood [2] which produces realistic results. Further it has the IMC and an independent Simulink implementation as meaningful distinctions from previous work. The one area in which work has been re-used is the implementation of the Extended Kalman Filter. This filter-is well understood but the potential remains for the re-production of errors. Future work should consider the filter for investigation.

7.2 Difficulties with the WecSim environment

Despite the author's best efforts the control system was not realised in the wecSim environment until the end of the project time frame. The issues with the environment arose from version differences between MATLAB version R2017b and R2018b. Most importantly, R2018b does not automatically update the cache file of the simulink model automatically, meaning that changes to the model do not take effect. This does not appear to be the case in R2017b, where the project supervisor's work was developed.

This issue was resolved by either manually or programmatically deleting the cache file between every simulation run to force an update. Future work should ideally find a way to restore the automatic cache-updating process.

Further versioning issues include changes to the syntax for the legend() command, and the incompatibility of the bemIO environment. Fixes for these issues are included in the project source code.

7.3 Existence of the drift problem

It is clear from table 6.4 that the Simple and Effective controller does not keep the float within physical constraints for most of the sea states tested. It is not clear from the table what the behaviour of the float looks like when it violates these constraints. Figure 7.2 shows an example from one case in which constraints were violated. The values for the positions are taken as the integral of the float's velocity with respect to time.

In both dimensions the amplitude of the oscillations is limited according to the method Ringwood proposed [2]. However, the mean of the oscillation is not constant in either case. In surge especially the mean drifts positive, occasionally staying at what appear to be new set-points. In the case of Heave the mean drifts negative, and more slowly. This drift behaviour is observed in all other tested sea states. It is not necessarily positive or negative and may change over the course of a single run.

Due to the simplistic nature of the State-Space model based simulation, and its distinctiveness from prior work, this is strong evidence for the existence of the drift problem.
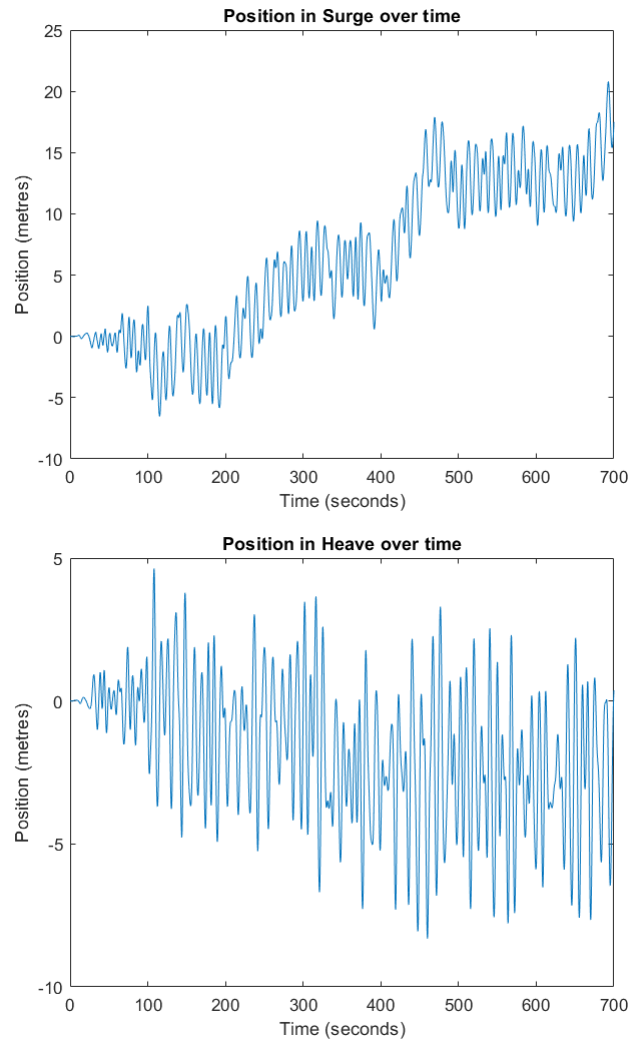
Figure 7.2: Graphs showing the position of the float in Surge (top) and Heave (bottom) during a simulation run. The input data was a sea-state with $H_s = 3$ and $T_e = 10$

7.4   Correcting Drift

The drift is caused by the fact that the integral of the velocity with respect to time has a non-zero average for short periods. This may be caused by the sea-state parameters changing over time, which causes a transition period for the system. In any case, the constraints proposed by ringwood are not sufficient to prevent this drift.

A hypothesis was proposed that the drift could be corrected with minimal impact on power generation using a small integral term. This term drives the mean of the float's velocity to 0, and by extension the mean of its position. Ringwood's constraint method could then be relied on to limit amplitude of the float's oscillation.

This hypothesis was tested using the implementation shown in figure 5.10, and produced the results shown in tables 6.5 and 6.6.

Physical constraints were not exceeded for any of the tested sea-states. The power generation has been positively affected in more violent sea states and reduced in gentler ones. The power gain in violent sea-states was an unintended result. The average mean power generated across all states was not significantly affected. Power gains in violent sea-states compensated for power lost in gentle sea-states.

Power may have been gained in gentler sea-states due to overshoot produced by the integral term. This would contradict Ringwood's assertion[2] that Simple and Effective control produces near-maximal power generation.

The unintended result and the simplicity of the model reduce the trust that should be put in these results. The hypothesis could not be refuted. This implies weak evidence that the drift problem can be rectified using this method.

7.5   Power Generation

Overall the results show that Simple and Effective control was able to produce more power than a passively damped, optimally tuned system in a majority of sea-states. It is also able to enforce physical constraints where the passive system might violate them due to a lack of control.

Power generation gains were most improved in gentle sea-states. Power generation improvements decreased as wave height and period increased, eventually generating less power than the passive system.

The average mean power improvement across all sea-states was 51%. This

figure is not as applicable as it may appear. In reality some sea-states are more common. This combined with the fact that power gain was improved for some sea-states and made worse for others means that any amount of power gain or loss over the passive model may be produced given different distributions of sea-states.

The WecSim implementation showed that even when the tracking performance was poor, some small amount of power was produced albeit much less than in the passive model.

Chapter 8

Conclusions

In this work the Simple and Effective control strategy proposed by Fusco and Ringwood[2] was adapted for a 6DOF WEC. The produced model was distinct from prior work by the project supervisor A.Hillis, making it useful for review. In particular the novel application of the Massay-Sain inverse algorithm has produced a robust inverse model of the WEC that is worth further study.

Due to difficulties with the WecSim simulation environment the state-space model originally used for development of the IMC was also used to model the WEC plant. This reduced the amount of the trust that can be assigned to positive results produced by this project. A crude version of the control system was eventually produced, and was found to have poor tracking performance whilst still generating a small amount of power. This suggests that the system's power production is not robust to model error, but that its stability is.

The first research question was whether the drift problem established by A. Hillis in prior work could be reproduced in an independently constructed model. It can.

The second research question was whether the drift issue could be resolved. Weak evidence was produced that it can be resolved using an integral feedback loop.

The final research question was how much power can be produced by this control strategy compared to a passively damped, optimally tuned system. It was shown that power production improvement of up to 162.2% is possible in gentle sea-states, but that power production is made worse during violent sea-states to keep the float within physical constraints. The worst power production loss over the passively damped system was -11.0%.

8.1　Future Work

Any future work using the Massay-Sain inverse method in this field should investigate its robustness against model error. This should be achieved within the WecSim environment or another well-established simulation environment.

The WecSim model produced in this project could be further developed to see if the presented results are still valid when fewer simplifying assumptions are made.

Alternative methods of correcting the float's position drift could be investigated. There is only weak evidence that the presented integral feedback loop is effective. There is a lack of theory to explain the effects that the loop had on the power generation of the system.

Bibliography

[1] Marine Power Systems, "Wave sub," accessed 24/11/2019. [Online]. Available: https://marinepowersystems.co.uk/wavesub/

[2] F. Fusco and J. Ringwood, "A simple and effective real-time controller for wave energy converters," *IEEE Transactions on Sustainable Energy, January*, vol. 4, no. 1, p. 2130, 2013.

[3] The European Marine Energy Center, "Wave clients," 2019, accessed 11/11/2019. [Online]. Available: http://www.emec.org.uk/about-us/wave-clients/

[4] S. Salter, "Wave power," *Nature*, vol. 249, p. 720 724, 1974.

[5] P. Aird, "Chapter 4 - deepwater metocean environments," in *Deepwater Drilling*, P. Aird, Ed. Gulf Professional Publishing, 2019, pp. 111 – 164. [Online]. Available: http://www.sciencedirect.com/science/article/pii/B9780081022825000041

[6] A. Hillis, "To appear. active control for multi-degree-of-freedom wave energy converters with load limiting."

[7] Carbon Trust, "Accelerating marine energy," Carbon Trust, Tech. Rep., Jul. 2011.

[8] e. a. National Renewable Energy Laboratory; National Technology and Engineering Solutions of Sandia, LLC (NTESS), "Wec-sim acknowledgements," [Online], 2014, accessed 15/04/2020.

[9] O. Abdelkhalik, "Multiresonant feedback control of a three-degree-of-freedom wave energy converter," *IEEE TRANSACTIONS ON SUSTAINABLE ENERGY*, vol. 8, no. 4, p. 15181527.

[10] ——, "Control of three degrees-of-freedom wave energy converters using pseudo-spectral methods," *ASME. J. Dyn. Sys., Meas., Control*, vol. 140, no. 7, p. 074501 9.

[11] D. Gorinevsky, "Ee392m: Control engineering in industry," accessed 26 November 2019]. [Online]. Available: https://web.stanford.edu/class/archive/ee/ee392m/ee392m.1056/

[12] S. Salter, "Wave energy: Nostalgic ramblings, future hopes and heretical suggestions," *J. Ocean Eng. Mar. Energy*, vol. 2, no. 4, p. 399428, 2016.

[13] D. Evans, D. Jeffrey, S. Salter, and J. Taylor, "Submerged cylinder wave energy device: theory and experiment," *Applied Ocean Research*, vol. 1, no. 1, p. 112.

[14] D. Evans, "A theory for wave-power absorption by oscillating bodies," *Journal of Fluid Mechanics*, vol. 77, no. 1, p. 125.

[15] A. Hillis and T. Appear, *The impact of modelling and prediction errors on the performance of optimally controlled multi-DOF wave energy converters.* Bath: s.n.

[16] H. Nguyen and P. Tona, "Wave excitation force estimation for wave energy converters of the point-absorber type," *IEEE TRANSACTIONS ON CONTROL SYSTEMS TECHNOLOGY*, vol. 26, no. 6, p. 21732181.

[17] *Proceedings of the European Wave and Tidal Energy Conference*, no. 13. Napoli, Italy: Technical Comittee of the European Wave and Tidal Energy Conference, Sep. 2019, iSSN 2309-1983.

[18] W. J. Pierson Jr. and L. Moskowitz, "A proposed spectral form for fully developed wind seas based on the similarity theory of s. a. kitaigorodskii," *Journal of Geophysical Research (1896-1977)*, vol. 69, no. 24, pp. 5181–5190, 1964. [Online]. Available: https://agupubs.onlinelibrary.wiley.com/doi/abs/10.1029/JZ069i024p05181

[19] J. H. G. M. Alves, M. L. Banner, and I. R. Young, "Revisiting the piersonmoskowitz asymptotic limits for fully developed wind waves," *Journal of Physical Oceanography*, vol. 33, no. 7, pp. 1301–1323, 2003. [Online]. Available: https://doi.org/10.1175/1520-0485(2003)033¡1301:RTPALF¿2.0.CO;2

[20] M. Sain and J. Massey, "Invertibility of linear time-invariant dynamical systems," *IEEE Transactions on Automatic Control*, vol. 14, no. 2, pp. 141–149, 1969.

[21] S. Sundaram, "Inversion of linear systems," Oct. 2004, iTR Seminar, University of Illinois at Urbana-Champaign. [Online]. Available: https://engineering.purdue.edu/ sundara2/talks/invert.pdf

[22] F. Fusco, "Real-time forecasting and control foroscillating wave energy devices," Ph.D. dissertation, National University of Ireland Meynooth, Jul. 2012.

Appendices

Appendix A

Radiation force Transfer Functions

In surge,

$$\frac{290679.29s^4 + 14649745.15s^3 + 26385215.63s^2 + 33911837.69s - 502286.47}{s^4 + 1.63s^3 + 4.42s^2 + 2.95s + 3.05}$$

In heave,

$$\frac{484147.09s^4 + 24299554.51s^3 + 40614156.16s^2 + 46679365.01s - 592668.23}{s^4 + 1.50s^3 + 3.77s^2 + 2.26s + 2.23}$$

Appendix B

Project code: inputFile.m - Written by Author

```matlab
1  %Run SSModel_calc.m to populate workspace.
2  SSModel_calc;
3  load('FEX_samples/FEX_8_6.mat') %Grab a demo FEX sample.
       Comment out if running batch process.
4
5  %Specify the excitation force sinusoid
6  % seaWave.amp = 1e6;s
7  % seaWave.freq = 0.4;
8
9  %Calculate the lookup table values
10 %Surge TF
11 %According to this Matlab Answers page, bode returns
       absolute values, not
12 %decibels: https://www.mathworks.com/matlabcentral/
       answers/90310-does-the-bode-function-automatically-
       converts-the-vector-points-into-decibels
13 load tfsurge_04numden.mat
14 surge.tf = tf(tfsurge_04num, tfsurge_04den);
15 surge.tf = surge.tf/(1.424e7/2.91e5);
16 [surge.amp,dummy,surge.freq] = bode(surge.tf);
17 surge.amp = squeeze(surge.amp);
18 surge.freq = squeeze(surge.freq);
19 clear dummy
20
21 %Heave TF
22 load tfheave_04numden.mat
```

61

```
23  heave.tf=tf(tfheave_04num,tfheave_04den);
24  heave.tf=heave.tf/(100/2);
25  [heave.amp,dummy,heave.freq] = bode(heave.tf);
26  heave.amp = squeeze(heave.amp);
27  heave.freq = squeeze(heave.freq);
28  clear dummy
29
30
31  % Construct the discrete inverse:
32  % L = 1; %L is 1 ! Don't forget this. Have proven
33  Ts = 0.02; %Time-step, remember to set in simulink as
        well.
34
35  SS_discrete = c2d(SS_full,Ts);
36
37  M0 = SS_discrete.D;
38  M1 = [              M0,                  zeros(length(M0),length(M0)
        );...
39          SS_discrete.C*SS_discrete.B,                     M0
                             ];
40
41  K = pinv(M1(:,1:6));
42
43  O_L = [SS_discrete.C;SS_discrete.C*SS_discrete.A]; %
        Observability of M1
44  SS_inverse.A = SS_discrete.A - (SS_discrete.B*K*O_L);
45  SS_inverse.B = SS_discrete.B*K;
46  SS_inverse.C = -K*O_L;
47  SS_inverse.D = K;
48  SS_inverse = ss(SS_inverse.A, SS_inverse.B,SS_inverse.C,
        SS_inverse.D,Ts);
49
50  %Due to discreteInverse being realisable in real time,
        the filter can be
51  %anything! It has uncancelled zeroes at:
52  %0.129 rads, 0.989+-0.128j for Heave
53  %0.131 rads, 0.989+-0.13j for Surge (Discrete time pzmap)
```

Appendix C

Project code: SSModel_calc.m - Written by A. Hillis

```matlab
1  %%%Calculate state−space model of float in static
       position
2  %%%Full scale
3  load('ssRadf.mat')
4
5  rho_sea=1000;
6  g=9.81;
7  % Float
8  depth = 2;                    % Depth to top of float
9  Des = 12;                     % Outer diameter of float
       shell [m]
10 R = Des/2;                    % Outer radius of float shell
        [m]
11 CylLength = 4.75;            % Length of cylinder between
       hemispheres [m]
12 reldenfloat = 0.8;           % Density of float reative to
        sea water [−]
13 rho_steel = 7850;            % Density of steel [kg/m^3]
14 alphaDeg = 45;                % deg xz−plane (zero if att
       point is on horizontal central line, 90 if on bottom
       og float)
15 betaDeg = 0;                  % deg xy−plane (zero if x
       value of att point is max (corner of cylinder) 90 y is
        max (peak of hemisphere))
```

```matlab
16  FloatCd = 0.5;
17  FloatCdVector = [FloatCd 100 FloatCd 200*FloatCd 0 200*
        FloatCd];% Drag coefficients in 6 degrees of freedom,
        4 and 6 picked at random to reduce yaw movement
18
19  % Reactor
20  ReactorD = 4.3;
21  ReactorCylLength = 35.7;                          % Only
        cylinder (excluding the two hemispheres)
22  ReactorWidth = 30;                               % From
        centre of tube to centre of tube
23  NetBuoyReactor = 101.9*10^3;                     % Net
        buoyancy of reactor [f kg] (Positive is buoyant)
24  ReactorDepth = 25.85;                            %
        Distance from mean sea surface to top of reactor (
        positive nr)
25  SeaDepth = 75;                                   %
        Distance from mean sea surface to seabed (positive nr)
26  ReactorCd = 0.5;
27  ReactorCdVector = [ReactorCd 100 ReactorCd 200*ReactorCd
        200*ReactorCd 200*ReactorCd];   % Drag coefficients in
         6 degrees of freedom, 4 and 6 picked at random to
        reduce yaw movement
28
29  %% Coordinates  (m, m, m)
30  % Tether line attachemnt point on float in global frame
31
32  alphaRad = alphaDeg*pi/180;
33  betaRad = betaDeg*pi/180;
34  % F1 = [R*cos(alphaRad)*cos(betaRad) R*cos(alphaRad)*sin(
        betaRad)+CylLength/2 -depth-R-R*sin(alphaRad)];      %
        Corner tether
35
36  %Transform to Float local frame - subtract float radius
        from z co-ord
37  %(Global frame at sea level)
38  F1 = [R*cos(alphaRad)*cos(betaRad) R*cos(alphaRad)*sin(
        betaRad)+CylLength/2 -R*sin(alphaRad)];     % Corner
        tether
39  F2 = [F1(1) -F1(2) F1(3)];      % Corner tether
40  F3 = [-F1(1) -F1(2) F1(3)];     % Corner tether
41  F4 = [-F1(1) F1(2) F1(3)];      % Corner tether
42  FC = [0 0 -depth-2*R];          % Central tether
43
44  % Tether line attachemnt point on reactor in global frame
45  T1 = [ReactorCylLength/2 ReactorWidth/2 -ReactorDepth+
```

```matlab
         depth+R];          % Corner tether transformed to relative
             to float COG
46   T2 = [T1(1) -T1(2) T1(3)];                    % Corner tether
47   T3 = [-T1(1) -T1(2) T1(3)];                   % Corner tether
48   T4 = [-T1(1) T1(2) T1(3)];                    % Corner tether
49   TC = [0  0  T1(3)];                           % Central tether
50   alfaXYT1F1 = abs(atan((T1(3)-F1(3))/((T1(1)-F1(1))^2+(T1
         (2)-F1(2))^2)^0.5));% PTO tether line [rad]
51   StiffnessCorner = 500*10^3;                   % Corner
         PTO tether stiffness coefficient [N/m]
52
53
54   %Calculate corner tether initial length
55   xyz_pto=T1-F1;
56   corner_line_init_length=(Des/2) + sqrt(xyz_pto(1)^2 +
         xyz_pto(2)^2 + xyz_pto(3)^2); %add radius of float -
         assume lines point to cob
57
58   %Vectors to float thether attachment points relative to
         float COG
59   N_01=[0 F1(3) -F1(2);-F1(3) 0 F1(1);F1(2) -F1(1) 0];
60   N_02=[0 F2(3) -F2(2);-F2(3) 0 F2(1);F2(2) -F2(1) 0];
61   N_03=[0 F3(3) -F3(2);-F3(3) 0 F3(1);F3(2) -F3(1) 0];
62   N_04=[0 F4(3) -F4(2);-F4(3) 0 F4(1);F4(2) -F4(1) 0];
63
64   %Vectors along PTO tethers
65   S1=F1-T1;
66   S2=F2-T2;
67   S3=F3-T3;
68   S4=F4-T4;
69
70   S_01=[0 S1(3) -S1(2);-S1(3) 0 S1(1);S1(2) -S1(1) 0];
71   S_02=[0 S2(3) -S2(2);-S2(3) 0 S2(1);S2(2) -S2(1) 0];
72   S_03=[0 S3(3) -S3(2);-S3(3) 0 S3(1);S3(2) -S3(1) 0];
73   S_04=[0 S4(3) -S4(2);-S4(3) 0 S4(1);S4(2) -S4(1) 0];
74
75   %Unit vectors along PTO tethers
76   e_s1=S1./norm(S1);
77   e_s2=S2./norm(S2);
78   e_s3=S3./norm(S3);
79   e_s4=S4./norm(S4);
80
81   %%%Calculate stiffness matrix
82
83   %% Preload
84   VolumeFloat =4/3*pi*(Des/2)^3 + pi*(Des/2)^2*CylLength;
```

```matlab
85  VolumeReactor =   1198.533;
                                                            % kg
       from .h5 file
86  Mdisplacedfloat = VolumeFloat*rho_sea;
                                                 % kg
87  Mdisplacedreactor = VolumeReactor*rho_sea;
                                                 % kg
88  Mfloat = reldenfloat*Mdisplacedfloat;
                                                    % kg
89  Mreactor=Mdisplacedreactor−NetBuoyReactor;
                                        % Net buoyancy of
       reactor [f kg]
90  Systemnetbuoyancy = (Mdisplacedfloat+Mdisplacedreactor−
       Mfloat−Mreactor)*g;   % N
91  TotalPreloadPTO = −(Mdisplacedfloat−Mfloat)*g;
                                     % N opposite of net
       buoyancy
92  PercentPreloadCentral = 0;                       % Percent
       of preload in central tether [%]
93  PreloadPTOCorner =   −((1−PercentPreloadCentral/100)*
       TotalPreloadPTO/4)/sin(alfaXYT1F1);  % Force aligned
       with tether line

95  G_0 = PreloadPTOCorner/norm(S1);   %All norms of Dxyz are
       the same as symettical

97  %%%%Kt for non colinear lines
98  G_01 = −[eye(3);N_01']*e_s1';
99  G_02 = −[eye(3);N_02']*e_s2';
100 G_03 = −[eye(3);N_03']*e_s3';
101 G_04 = −[eye(3);N_04']*e_s4';

103 Kt1 = [(StiffnessCorner−G_0)*(G_01)*(G_01') + G_0*[eye(3)
       ;N_01']*[eye(3) N_01] + [zeros(3,3) zeros(3,3); zeros
       (3,3) G_0*S_01*N_01]];
104 Kt2 = [(StiffnessCorner−G_0)*(G_02)*(G_02') + G_0*[eye(3)
       ;N_02']*[eye(3) N_02] + [zeros(3,3) zeros(3,3); zeros
       (3,3) G_0*S_02*N_02]];
105 Kt3 = [(StiffnessCorner−G_0)*(G_03)*(G_03') + G_0*[eye(3)
       ;N_03']*[eye(3) N_03] + [zeros(3,3) zeros(3,3); zeros
       (3,3) G_0*S_03*N_03]];
106 Kt4 = [(StiffnessCorner−G_0)*(G_04)*(G_04') + G_0*[eye(3)
       ;N_04']*[eye(3) N_04] + [zeros(3,3) zeros(3,3); zeros
       (3,3) G_0*S_04*N_04]];
107 Kt = Kt1 + Kt2 + Kt3 + Kt4;
108
```

```matlab
109  %Inverse kinematic Jacobian
110  L = -[G_01 G_02 G_03 G_04]';
111
112  %Radiation state space model derived from 4th order
         transfer function fits.
113  %From 4th order optimisation, observable canonical form
114  load tfsurge_04numden.mat
115  G_surge = tf(tfsurge_04num, tfsurge_04den);
116  G_surge = G_surge/(1.424e7/2.91e5);
117  Gsden = G_surge.den{1};
118  Gsnum = G_surge.num{1};
119  Gsden = Gsden./Gsden(1);
120  Gsnum = Gsnum./Gsden(1);
121  Ars = [0 1 0 0;
122         0 0 1 0;
123         0 0 0 1;
124         -fliplr(Gsden(2:end))];
125
126  Brs = [0 0 0 1.2e-3]';
127
128  Crs = fliplr([Gsnum(2:end-1) 0]);
129
130  load tfheave_04numden.mat
131  G_heave=tf(tfheave_04num, tfheave_04den);
132  G_heave=G_heave/(100/2);
133  Ghden = G_heave.den{1};
134  Ghnum = G_heave.num{1};
135  Ghden = Ghden./Ghden(1);
136  Ghnum = Ghnum./Ghden(1);
137  Arh = [0 1 0 0;
138         0 0 1 0;
139         0 0 0 1;
140         -fliplr(Ghden(2:end))];
141
142  Ar_blank = [0 1 0 0;
143         0 0 1 0;
144         0 0 0 1;
145         zeros(1,4)].*1;
146
147  Brh = [0 0 0 1.2e-3]';
148
149  Crh = fliplr([Ghnum(2:end-1) 0]);
150
151  %Form complete radiation state space model for all DOFs (
         but only include
152  %surge and heave)
```

```matlab
153  Ar = blkdiag(Ars, Ar_blank, Arh, Ar_blank, Ar_blank,
         Ar_blank);
154  Br = blkdiag(Brs, zeros(size(Brs)), Brh, zeros(size(Brs))
         , zeros(size(Brs)), zeros(size(Brs)));
155  Cr = blkdiag(Crs, zeros(size(Crs)), Crh, zeros(size(Crs))
         , zeros(size(Crs)), zeros(size(Crs)));
156  Dr = zeros(6,6);
157
158  %%%Mass and added mass
159  M = diag([body(1).mass body(1).mass body(1).mass body(1).
         momOfInertia]);
160  Ainf = body(1).hydroForce.fAddedMass(:,1:6);
161
162  Bv = body(1).hydroForce.visDrag;
163  %%ADD PTO DAMPING IF INCLUDED
164  % Bv=Bv+diag([250*10^3 250*10^3 250*10^3 250*10^3
         250*10^3 250*10^3]);
165
166  %%%Adjust Bv for linearised viscous drag approximation -
         based on emprical
167  %%%tuning with no control force
168  Bv_adj=ones(6,6).*1;
169  Bv = Bv.*Bv_adj;
170  %%%Add some damping to pitch-pitch mode to aid controller
          design
171  Bv(5,5)=Bv(6,6)./1e2;
172
173  %%%Create augmented ss matrices including radiation
174  A_wec = [zeros(6,6) eye(6) zeros(size(Cr)); -(M + Ainf)\
         Kt -(M + Ainf)\Bv -(M + Ainf)\Cr; zeros(size(Br)) Br
         Ar];
175  B_wec = [zeros(6,6); inv(M + Ainf); zeros(size(Br))];
176  % C_wec = [eye(12) zeros(12,24)];
177  C_wec = [zeros(6,6) eye(6) zeros(size(Cr))];
178  D_wec=0;
179
180  SS_full=ss(A_wec,B_wec,C_wec,D_wec); %This has 144 states
          including radiation damping in all modes
181
182  %remove non-relevant poles
183
184  %remove using balreal and modred
185  [SYSB,G] = balreal(SS_full);
186  elim = (G<1e-8);              % small entries of g ->
         negligible states
187  SYS_min = modred(SYSB, elim);  % remove negligible states
```

```matlab
188
189 %without radiation: This one is used with LQRY as other
        models do not find
190 %feasible solution. Radiation damping is not too
        significant anyway.
191 A_wec_nr = [zeros(6,6) eye(6); -(M + Ainf)\Kt -(M + Ainf)
        \Bv];
192 B_wec_nr = [zeros(6,6); inv(M + Ainf)];
193 C_wec_nr = [zeros(6,6) eye(6)];
194 D_wec_nr = zeros(6,6);
```

Appendix D

EKF Code - Written by A. Hillis

```matlab
1  function [Amplitude, Phase, Frequency]   = EKF_narrowband
       (y)
2  coder.extrinsic('evalin')
3  % Initialization
4  persistent P;
5  persistent x;
6
7  dt = 0; %edit this to match your timestep
8  dt = evalin('base','Ts');
9  if isempty(P)
10     x = [0 0 0.1]';        %state estimate
11     P = diag([1e0 1e0 1e0]);    %Covariance matrix
12 end
13
14 %%%%%%%%%%%From Fusco thesis%%%%%%%%%%%%%%%%%%%%%%
15 %%%State vector X = [a theta w]
16 x1 = x(1);   %Amplitude
17 x2 = x(2);   %Phase
18 w = x(3);    %frequency
19
20 %State transition matrices
21 A = [cos(w*dt)  sin(w*dt)  0;
22      -sin(w*dt)  cos(w*dt)  0;
23      0 0 1];
24
25 q1 = 1e12; q2 = 1e-1; q3 = 1e-2;%Must be comparable to
```

```matlab
         expected  magnitudes  of  each  state
26
27  % q = [rand*q1 rand*q2 rand*q3]';
28  % Q = diag(q);
29  % R=rand*0.1;
30
31  q = [q1 q2 q3]';
32  Q = diag(q);
33  R=1e-1; %Measurement  noise
34
35  %Jacobian
36  dA = [cos(w*dt) sin(w*dt) (-dt*x1*sin(w*dt) + dt*x2*cos(w
         *dt));
37        -sin(w*dt) cos(w*dt) (-dt*x1*cos(w*dt) - dt*x2*sin(w*
              dt));
38         0 0 1];
39  F = [(x1*cos(w*dt) + x2*sin(w*dt)); (-x1*sin(w*dt) + x2*
         cos(w*dt)); w];
40  C = [1 0 0];
41
42  %EKF predict/correct
43  x = A*x;
44  P = dA*P*dA' + Q;
45
46  S = C*P*C' + R;
47  K = P*C'/S;
48  x = x + K*(y-C*x);
49  P = (eye(3) - K*C)*P;
50
51  %outputs
52  Amplitude = sqrt(x(1)^2 + x(2)^2);
53  Frequency = x(3);
54  Phase = x(2);
```

Appendix E

Github Link

https://github.com/SELIG-C/FYP-2020